

---

Zdeněk Stuchlík · Andrea Kotrlová

# Orbital resonances in discs around braneworld Kerr black holes

**Abstract** Rotating black holes in the brany universe of the Randall–Sundrum type with infinite additional dimension are described by the Kerr geometry with a tidal charge  $b$  representing the interaction of the brany black hole and the bulk spacetime. For  $b < 0$  rotating black holes with dimensionless spin  $a > 1$  are allowed. We investigate the role of the tidal charge in the orbital resonance model of quasiperiodic oscillations (QPOs) in black hole systems. The orbital Keplerian frequency  $\nu_K$  and the radial and vertical epicyclic frequencies  $\nu_r$ ,  $\nu_\theta$  of the equatorial, quasicircular geodesical motion are given. Their radial profiles related to Keplerian accretion discs are discussed, assuming the inner edge of the disc located at the innermost stable circular geodesic. For completeness, naked singularity spacetimes are considered too. The resonant conditions are given in three astrophysically relevant situations: for direct (parametric) resonances of the oscillations with the radial and vertical epicyclic frequencies, for the relativistic precession model, and for some trapped oscillations of the warped discs, with resonant combinational frequencies involving the Keplerian and radial epicyclic frequencies. It is shown, how the tidal charge could influence matching of the observational data indicating the 3:2 frequency ratio observed in GRS 1915+105 microquasar with prediction of the orbital resonance model; limits on allowed range of the black hole parameters  $a$  and  $b$  are established. The “magic” dimensionless black hole spin enabling presence of strong resonant phenomena at the radius, where  $\nu_K : \nu_\theta : \nu_r = 3 : 2 : 1$ , is determined in dependence on the tidal charge. Such strong resonances could be relevant even in sources with highly scattered resonant frequencies, as those expected in Sgr A\*. The specific values of the spin and tidal charge are given also for existence of specific radius where  $\nu_K : \nu_\theta : \nu_r = s : t : u$  with  $5 \geq s > t > u$  being small natural numbers. It is shown that for some ratios such situation is impossible in the field of black holes. We can conclude that analysing the microquasars high-frequency QPOs in the framework of orbital resonance models, we can put relevant limits on the tidal charge of brany Kerr black holes.

**Keywords** Accretion; accretion disks · Braneworld black hole physics · Orbital resonances · X-rays: general

**PACS** 97.10.Gz · 04.70.-s · 04.50.Gh · 97.80.Jp

## 1 Introduction

In recent years, one of the most promising approaches to the higher-dimensional gravity theories seems to be the string theory and M-theory describing gravity as a truly higher-dimensional interaction becoming effectively 4D at low enough energies and these theories inspired braneworld models, where the observable universe is a 3-brane (domain wall) to which the standard-model (non-gravitational) matter fields are confined, while gravity field enters the extra spatial dimensions, the size of which may be much larger than the Planck length scale  $l_p \sim 10^{-33}$  cm [9]. The braneworld models could therefore provide an elegant solution

to the hierarchy problem of the electroweak and quantum gravity scales, as these scales become to be of the same order ( $\sim \text{TeV}$ ) due to large scale extra dimensions [9]. Therefore, future collider experiments can test the braneworld models quite well, including the hypothetical mini black hole production on the TeV-energy scales [27, 25]. On the other hand, the braneworld models could be observationally tested since they influence astrophysically important properties of black holes.

Gravity can be localized near the brane at low energies even with a non-compact, infinite size extra dimension with the warped spacetime satisfying the 5D Einstein equations with negative cosmological constant as shown by Randall and Sundrum [59]. Then an arbitrary energy-momentum tensor could be allowed on the brane [67].

The Randall–Sundrum model gives the 4D Einstein gravity in low energy limit, and the conventional potential of weak, Newtonian gravity appears on the 3-brane with high accuracy. Significant deviations from the Einstein gravity occur at very high energies, e.g., in the very early universe, and in vicinity of compact objects (see, e.g., [23, 49, 29, 8]). Gravitational collapse of matter trapped on the brane results in black holes mainly localized on the brane, but their horizon could be extended into the extra dimension. The high-energy effects produced by the gravitational collapse are disconnected from the outside space by the horizon, but they could have a signature on the brane, influencing properties of black holes [49]. There are high-energy effects of local character influencing pressure in collapsing matter, and also non-local corrections of “back-reaction” character arising from the influence of the Weyl curvature of the bulk space on the brane – the matter on the brane induces Weyl curvature in the bulk which makes influence on the structures on the brane due to the bulk graviton stresses [49]. The combination of high-energy (local) and bulk stress (non-local) effects alters significantly the matching problem on the brane, as compared to the 4D Einstein gravity; for spherical objects, matching no longer leads to a Schwarzschild exterior in general [23, 29]. Moreover, the Weyl stresses induced by bulk gravitons imply that the matching conditions do not have unique solution on the brane; in fact, knowledge of the 5D Weyl tensor is needed as a minimum condition for uniqueness [29].<sup>1</sup>

There are two kinds of black hole solutions in the Randall–Sundrum braneworld model with infinite extension of the extra dimension. One kind of these solutions looks like black string from the viewpoint of an observer in the bulk, while being described by the Schwarzschild metric for matter trapped on the brane [20]. The generalizations to rotating black string solution [55] and solutions with dilatonic field [57] were also found. However, the black string solutions have curvature singularities at infinite extension along the extra dimension [7]. There is a proposal that the black hole strings could evolve to localized black cigar solutions due to the classical instability near the anti-de Sitter horizon [20, 31], but it is not resolved at present [35, 8].

Second kind of these solutions representing a promising way of generating exact localized solutions in the Randall–Sundrum braneworld models was initiated by Maartens and his coworkers [49, 29, 23]. Assuming spherically symmetric metric induced on the 3-brane, the effective gravitational field equations on the brane could be solved, giving Reissner–Nordström static black hole solutions endowed with a “tidal” charge parameter  $b$  instead of the standard electric charge parameter  $Q^2$  [23]. The tidal charge reflects the effects of the Weyl curvature of the bulk space, i.e., from the 5D graviton stresses with bulk graviton tidal effect giving the name of the charge [23, 49]. Note that the tidal charge can be both positive and negative, and there are some indications that the negative tidal charge should properly represent the “back-reaction” effects of the bulk space Weyl tensor on the brane [49, 23, 63].

The exact stationary and axisymmetric solutions describing rotating black holes localized in the Randall–Sundrum braneworld were derived in [8]. They are described by the metric tensor of the Kerr–Newman form with a tidal charge representing the 5D correction term generated by the 5D Weyl tensor stresses. The tidal charge has an “electric” character again and arises due to the 5D gravitational coupling between the brane and the bulk, reflected on the brane through the “electric” part of the bulk Weyl tensor [8], in close analogy with the spherically symmetric case [23].

When both the tidal and electric charge are present in a brany black hole, its character is much more complex and usual Kerr–Newman form of the metric tensor is allowed only in the approximate case of small values of the rotation parameter  $a$ . For linear approximation in  $a$ , the metric arrives at the usual Boyer–Lindquist form describing “tidally” charged and slowly rotating brany black holes [8]. For large rotational parameters, when the linear approximation is no longer valid, additional off-diagonal metric components  $g_{r\phi}$ ,  $g_{rt}$  are relevant along with the standard  $g_{\phi t}$  component due to the combined effects of the local bulk on the brane and the dragging effect of rotation, which through the “squared” energy momentum tensor on the brane distort the event horizon that becomes a stack of non-uniformly rotating null circles having different radii at

---

<sup>1</sup> At present, no exact 5D solution in the braneworld model is known.

fixed  $\theta$  while going from the equatorial plane to the poles [8]. In the absence of rotation, the metric tensor reduces to the Reissner–Nordström form with correction terms of local and non-local origin [21].

Here we restrict attention to the Kerr–Newman type of solutions describing the brany rotating black holes with no electric charge, when the results obtained in analysing the behaviour of test particles and photons or test fields around the Kerr–Newman black holes could be used assuming both positive and negative values of the brany tidal parameter  $b$  (used instead of the charge parameter  $Q^2$ ) [54].

It is very important to test the role of the hypothetical tidal charge, implied by the theory of multidimensional black holes in the Randall–Sundrum braneworld with non-compactified additional space dimension, in astrophysical situations, namely in the accretion processes and related optical phenomena, including the oscillatory features observed in the black hole systems. There are two complementary reasons for such studies. First, the observational data from the black hole systems (both Galactic binary systems or Sgr A\* and active galactic nuclei) could restrict the allowed values of the tidal charge, giving a relevant information on the properties of the bulk spacetime and putting useful additional limits on the elementary particle physics. Second, the presence of the tidal charge could help much in detailed understanding of some possible discrepancies in the black hole parameter estimates coming from observational data that are obtained using different aspects of modelling accretion phenomena [81, 50].

In fact, the black hole parameter estimates come from a variety of astrophysical observations [41, 42, 51, 60, 61, 50]. The black hole spin estimates are commonly given by the optical methods, namely by X-ray line profiles [48, 36, 26, 28, 86, 87] and X-ray continuum spectra [52, 53, 66], and by quasiperiodic oscillations, the frequency of which enable, in principle, the most precise spin estimates, because of high precision of the frequency measurements.<sup>2</sup>

Therefore, we discuss here in detail the orbital resonance model of QPOs, which seems to be the most promising in explaining the observational data from four microquasars, namely GRO J1655-40, XTE 1550-564, H 1743-322, GRS 1915+105 [80, 76, 77, 75] and in Sgr A\* [11, 13, 76], or some extragalactic sources as NGC 5408 X-1 [70].

It is well known that in astrophysically relevant situations the electric charge of a black hole becomes zero or negligible on short time scales because of its neutralization by accreting preferentially oppositely charged particles from ionized matter of the accretion disc [88, 54, 24]. Clearly, this statement remains true in the braneworld model, and that is the reason why it is enough to consider properties of brany Kerr black holes endowed with a tidal charge only. Of course, the tidal charge reflecting the non-local gravitational effects of the bulk space is non-negligible in general and it can have quite strong effect on the physical processes in vicinity of the black hole. Recently, some authors tested the tidal charge effects in the weak field limit for optical lensing [40] and relativistic precession or time delay effect [17]. Here we develop a framework of testing the tidal charge effects in the strong field near black holes with accretion discs giving rise to kHz QPOs.

In Section 2, the Kerr black holes with a tidal charge, introduced by Aliev and Gümrükçüoğlu [8], are described and their properties are briefly summarized. In Section 3, the Carter equations of motion are given, the equatorial circular geodesics, i.e., Keplerian circular orbits reflecting properties of thin accretion discs, are determined and properties of photon circular orbits and innermost stable orbits are discussed. In Section 4, the radial and vertical (latitudinal) epicyclic frequencies  $\nu_r$  and  $\nu_\theta$ , together with the Keplerian orbital frequency  $\nu_K$ , are given. In Section 5, their properties are discussed, namely their radial profiles through the Keplerian accretion disc with its inner radius assumed to be located at the radius of the innermost stable circular geodesic, where the radial epicyclic frequency vanishes. In Section 6, we shortly discuss the resonance conditions for the direct resonance of the both epicyclic frequencies ( $\nu_\theta : \nu_r = 3 : 2$ ) assumed to be in a parametric resonance [80], the relativistic precession model [69] where we assume a resonance of oscillations with  $\nu_K : (\nu_K - \nu_r) = 3 : 2$ , and the resonance of trapped oscillations assumed in warped disc as discussed by Kato [38] [ $(2\nu_K - \nu_r) : 2(\nu_K - \nu_r) = 3 : 2$ ]. In Section 7 we determine the “magic” (dimensionless) spin of brany Kerr black holes in dependence on the (dimensionless) tidal charge, enabling presence of strong resonant phenomena because of the very special frequency ratio  $\nu_K : \nu_\theta : \nu_r = 3 : 2 : 1$ ; possibility of other small integer ratios of the three frequencies at a shared radius is also discussed. Concluding remarks on the resonant phenomena in strong gravity of brany black holes are presented in Section 8.

---

<sup>2</sup> But see some problems connected with the wide variety of the resonance models [80].

## 2 Braneworld Kerr black holes

Using the Gauss–Codazzi projective approach, the effective gravitational field equations on a 3-brane in a 5D bulk spacetime can be defined [10, 67]. The self-consistent solutions of the effective 4D Einstein equations on the brane require the knowledge of the non-local gravitational and energy-momentum terms coming from the bulk spacetime. Therefore, the brany field equations are not closed in general and evolution equations into the bulk have to be solved for the projected bulk curvature and energy-momentum tensors [7]. However, in particular cases the brany-equations system could be made closed assuming a special ansatz for the induced metric. In this way, both spherically symmetric [23] and axially symmetric brany black hole spacetimes [8] have been found.

Under the assumption of stationary and axisymmetric Kerr–Schild metric on the brane and supposing empty bulk space and no matter fields on the brane ( $T_{\alpha\beta} = 0$ ) [8] the effective Einstein equations on the brane reduce to the form  $R_{\alpha\beta} = -E_{\alpha\beta}$ , where

$$E_{\alpha\beta} = {}^{(5)}C_{ABCD} n^A n^C e_\alpha^B e_\beta^D \quad (1)$$

is the projected “electric” part of the 5D Weyl tensor  $C_{ABCD}$  used to describe the non-local gravitational effects of the bulk space onto the brane [8].

The line element for the brany rotating black holes can then be expressed in the standard Boyer–Lindquist coordinates and geometric units ( $c = G = 1$ ) in the form [8]

$$\begin{aligned} ds^2 = & - \left( 1 - \frac{2Mr - b}{\Sigma} \right) dt^2 - \frac{2a(2Mr - b)}{\Sigma} \sin^2 \theta dt d\phi \\ & + \frac{\Sigma}{\Delta} dr^2 + \Sigma d\theta^2 + \left( r^2 + a^2 + \frac{2Mr - b}{\Sigma} a^2 \sin^2 \theta \right) \sin^2 \theta d\phi^2, \end{aligned} \quad (2)$$

where

$$\Delta = r^2 + a^2 - 2Mr + b, \quad (3)$$

$$\Sigma = r^2 + a^2 \cos^2 \theta. \quad (4)$$

We can see that this metric looks exactly like the Kerr–Newman solution in general relativity [54], in which the square of the electric charge  $Q^2$  is replaced by a tidal charge parameter  $b$  (or “brany” parameter). Since the metric is asymptotically flat, by passing to the far-field regime we can interpret the parameter  $M$  as the total mass of the black hole and parameter  $a$  as the specific angular momentum (the black hole spin).

The event horizons of the spacetime are determined by the condition  $\Delta = 0$ . The radius of the outer event horizon is given by the relation

$$r_+ = M + \sqrt{M^2 - a^2 - b}. \quad (5)$$

The horizon structure depends on the sign of the tidal charge. We see that, in contrast to its positive values, the negative tidal charge tends to increase the horizon radius (see, e.g., Fig. 1).

The event horizon does exist provided that

$$M^2 \geq a^2 + b, \quad (6)$$

where the equality corresponds to the family of extreme black holes. It is clear that the positive tidal charge acts to weaken the gravitational field and we have the same horizon structure as in the usual Kerr–Newman solution. However, new interesting features arise for the negative tidal charge. For  $b < 0$  and  $a \rightarrow M$  it follows from equation (5) that the horizon radius

$$r_+ \rightarrow \left( M + \sqrt{-b} \right) > M; \quad (7)$$

such a situation is not allowed in the framework of general relativity. From equations (5) and (6) we can see that for  $b < 0$ , the extreme horizon  $r_+ = M$  corresponds to a black hole with rotation parameter  $a$  greater than its mass  $M$  (e.g., for extreme black hole with  $b = -M^2$  we have  $a = \sqrt{2}M$ ). Thus, the bulk effects on the brane may provide a mechanism for spinning up the black hole on the brane so that its rotation parameter exceeds

its mass. Such a mechanism is impossible in general relativity. Further, if the inner horizon determined by the formula

$$r_- = M - \sqrt{M^2 - a^2 - b} \quad (8)$$

turns out to be negative (it is possible for  $b < 0$ , again), the physical singularity ( $r = 0$ ,  $\theta = \pi/2$ ) is expected to be of space-like character, contrary to the case of  $b > 0$ , when it is of time-like character [23].

### 3 Geodesic motion

Motion of a test particle of mass  $m$  is given by the standard geodesic equation

$$\frac{Dp^\mu}{d\tau} = 0 \quad (9)$$

accompanied by the normalization condition  $p_\mu p^\mu = -m^2$  and can be treated in full analogy with the Kerr case [18]. There are three motion constants given by the spacetime symmetry – the energy being related to the Killing vector field  $\partial/\partial t$ , the axial angular momentum being related to the Killing vector field  $\partial/\partial\phi$ , and the angular momentum constant related to the hidden symmetry of the Kerr spacetime [19]. The geodesic equations could then be fully separated and integrated using the Hamilton–Jacobi method [19].

For the motion restricted to the equatorial plane ( $\theta = \pi/2$ ), the Carter equations take the form

$$\frac{d\theta}{d\lambda} = 0, \quad (10)$$

$$r^2 \frac{dr}{d\lambda} = \pm \sqrt{R(r)}, \quad (11)$$

$$r^2 \frac{d\phi}{d\lambda} = -(aE - L) + \frac{aP(r)}{\Delta}, \quad (12)$$

$$r^2 \frac{dt}{d\lambda} = -a(aE - L) + \frac{(r^2 + a^2)P(r)}{\Delta}, \quad (13)$$

where

$$P(r) = E(r^2 + a^2) - La, \quad (14)$$

$$R(r) = P(r)^2 - \Delta [m^2 r^2 + (aE - L)^2]. \quad (15)$$

The proper time of the particle  $\tau$  is related to the affine parameter  $\lambda$  by  $\tau = m\lambda$ . The constants of motion are: energy  $E$  and axial angular momentum  $L$  of the test particle in infinity (related to the stationarity and the axial symmetry of the geometry); for the equatorial motion, the third constant of motion  $Q = 0$  [19].

The equatorial circular orbits can most easily be determined by solving simultaneously the equations

$$R(r) = 0, \quad \frac{dR}{dr} = 0. \quad (16)$$

The specific energy and the specific angular momentum of the circular motion at a given radius are then determined by the relations [8, 22]

$$\frac{E}{m} = \frac{r^2 - 2Mr + b \pm a\sqrt{Mr - b}}{r(r^2 - 3Mr + 2b \pm 2a\sqrt{Mr - b})^{1/2}}, \quad (17)$$

$$\frac{L}{m} = \pm \frac{\sqrt{Mr - b}(r^2 + a^2 \mp 2a\sqrt{Mr - b}) \mp ab}{r(r^2 - 3Mr + 2b \pm 2a\sqrt{Mr - b})^{1/2}}. \quad (18)$$

Here and in the following, the upper sign corresponds to the corotating orbits ( $L > 0$ ), while the lower sign implies retrograde, counterrotating ( $L < 0$ ) motion of the particles.

In the analysis of the epicyclic frequency profiles, it is useful to relate the profiles to the photon circular geodesic and innermost stable circular geodesic radii (or innermost bound circular radii in case of thick disc

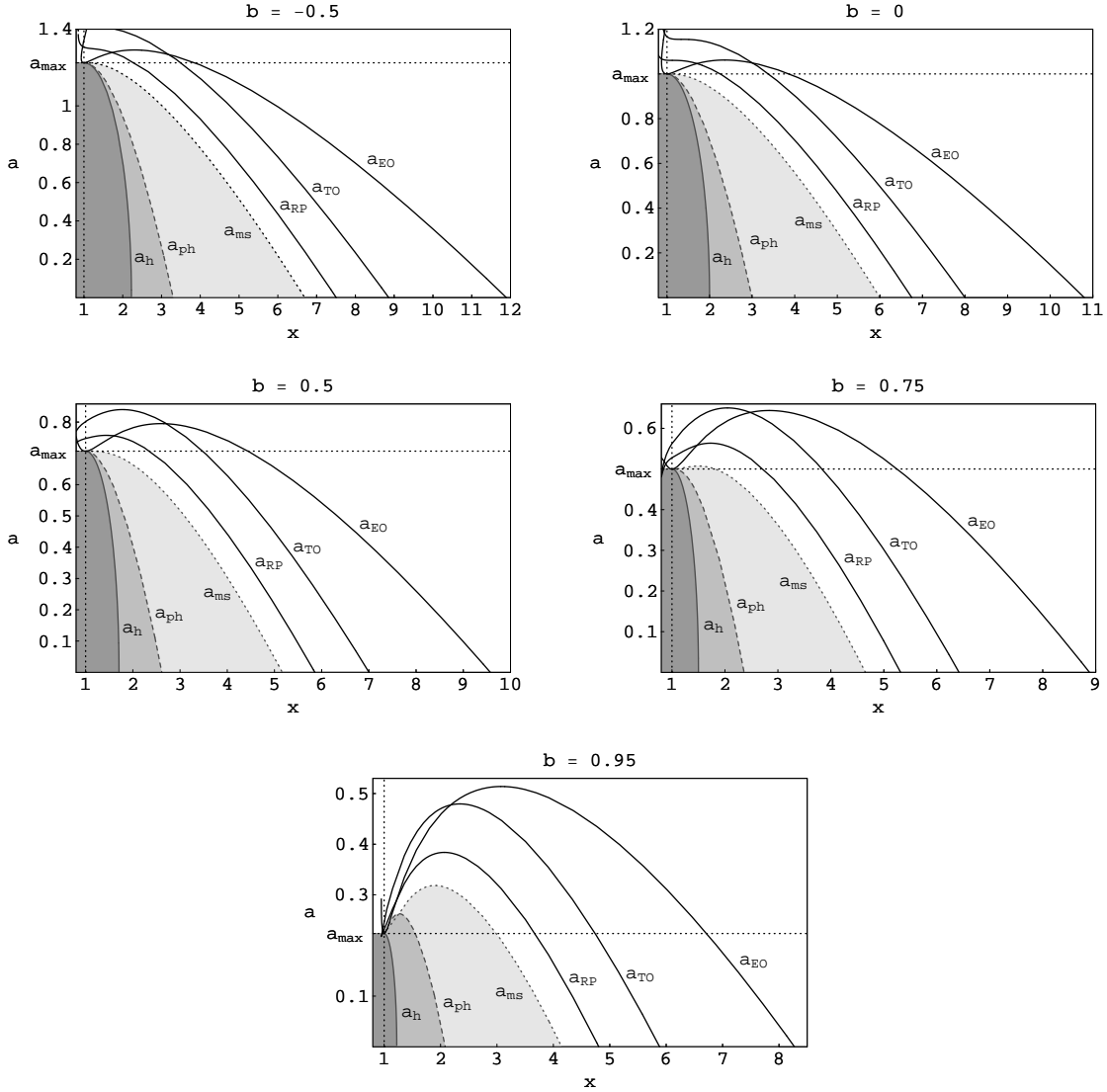


**Fig. 1** The behaviour of functions  $a_h$  (gray solid line),  $a_{ph}$  (gray dashed line) and  $a_{ms}$  (gray dotted line) that implicitly determine the radius of the outer event black hole horizon, the limiting photon orbit and the marginally stable circular orbit in the equatorial plane ( $\theta = \pi/2$ ) of a rotating black hole with a fixed value of the tidal charge  $b$ . The functions  $a_{EO} = a_{3:2}^{\theta/r}$ ,  $a_{RP} = a_{3:2}^{K/(K-r)}$  and  $a_{TO} = a_{3:2}^{(2K-r)/(2K-2r)}$  (black solid lines) represent the radii where the direct Epicyclic Oscillations resonance  $\nu_\theta : \nu_r = 3:2$ , the Relativistic Precession resonance  $\nu_K : (\nu_K - \nu_r) = 3:2$  and the Trapped Oscillations resonance  $(2\nu_K - \nu_r) : 2(\nu_K - \nu_r) = 3:2$  occur.

that is not considered here) that are relevant in discussions of properties of the accretion discs and their oscillations. Therefore, we put the limiting radii in an appropriate form.

For simplicity, hereafter we use dimensionless radial coordinate

$$x = r/M \quad (19)$$

and putting  $M = 1$ , we also use dimensionless spin  $a$  and brany parameter  $b$ . The outer event horizon  $x_h(a, b)$  is then implicitly determined by the relation

$$a = a_h(x, b) \equiv \sqrt{2x - x^2 - b}. \quad (20)$$

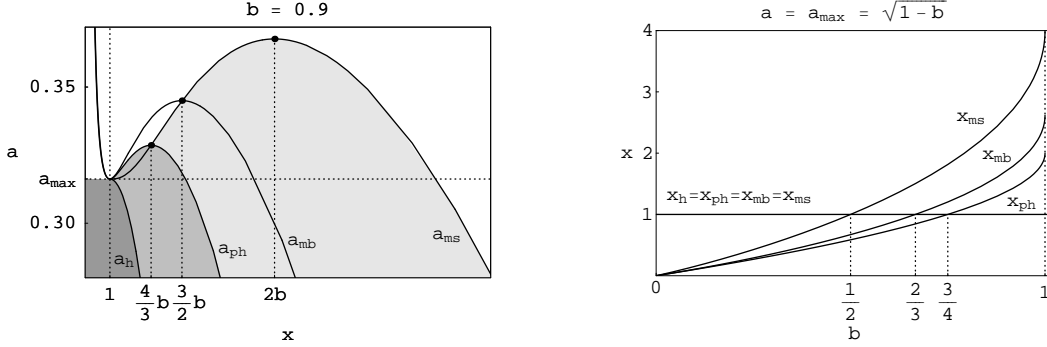


**Fig. 2** *Left panel:* The functions  $a_h$ ,  $a_{ph}$ ,  $a_{mb}$  and  $a_{ms}$  that implicitly determine the radii of the outer event black hole horizon, the limiting photon orbit and the marginally bound and stable circular orbits. The *right panel* illustrates the behaviour of the photon orbit  $x_{ph}$ , marginally bound  $x_{mb}$  and marginally stable  $x_{ms}$  orbits for the extreme black holes with  $0 \leq b \leq 1$ . The radii of the orbits that are situated at  $x < 1$  are out of our interest being located under the outer event black hole horizon.

Focusing our attention to the corotating orbits, we find the radius of the photon circular orbit  $x_{ph}(a, b)$  to be given by the relation

$$a = a_{ph}(x, b) \equiv \frac{x(3-x) - 2b}{2\sqrt{x-b}}, \quad (21)$$

the radius of the marginally bound orbit  $x_{mb}(a, b)$  to be given by

$$a = a_{mb}(x, b) \equiv \frac{\sqrt{x-b}(2x-b \mp x\sqrt{x})}{x-b}, \quad (22)$$

and the radius of the marginally stable corotating orbit  $x_{ms}(a, b)$  by the equation<sup>3</sup>

$$a = a_{ms}(x, b) \equiv \frac{4(x-b)^{3/2} \mp x\sqrt{3x^2 - 2x(1+2b) + 3b}}{3x-4b}; \quad (23)$$

for extreme black holes the maximum value of the black hole spin is

$$a_{\max} = \sqrt{1-b}, \quad (24)$$

thus, e.g., for  $b = -1$  we have  $a_{\max} = \sqrt{2}$ .

The function  $a_{ph}$  (21) has a local maximum at  $x = 1$  for brany parameter  $b \leq 3/4$  and a local maximum at  $x = \mathcal{X}_K = 4b/3$  for  $b > 3/4$  corresponding to the naked singularity spacetimes since  $a_{ph}(x = \mathcal{X}_K) > a_{\max}$ . The function  $a_{mb}$  (22) has a local maximum at  $x = 1$  for  $b \leq 2/3$  and at  $x = 3b/2$  for  $b > 2/3$ . The function  $a_{ms}$  (23) has a local maximum at  $x = 1$  for  $b \leq 1/2$  and at  $x = 2b$  for  $b > 1/2$  (this local maximum appears again only for naked singularities, since  $a > a_{\max}$ ). So, for  $x > 1$  the functions  $a_{ph}(x, b)$ ,  $a_{mb}(x, b)$  and  $a_{ms}(x, b)$  are not monotonically decreasing functions of radius for the whole range of the brany tidal charge parameter  $b$ , as usual in Kerr spacetimes. This special behaviour of  $a_{ph}$ ,  $a_{mb}$  and  $a_{ms}$  implies that for some values of the brany parameter  $b$  of extreme braneworld Kerr black holes the radial Boyer-Lindquist coordinates of the photon orbit  $x_{ph}$ , the marginally bound  $x_{mb}$  and marginally stable  $x_{ms}$  orbits do not merge with the black hole horizon radial coordinate at  $x_h = 1$ , as usual in Kerr spacetimes and are shifted to higher radii. There is

$$x_{ph}(a_{ph}, b) > 1 \quad \text{for} \quad 3/4 < b < 1, \quad (25)$$

$$x_{mb}(a_{mb}, b) > 1 \quad \text{for} \quad 2/3 < b < 1, \quad (26)$$

$$x_{ms}(a_{ms}, b) > 1 \quad \text{for} \quad 1/2 < b < 1. \quad (27)$$

For typical values of the tidal charge  $b$  the functions  $a_{ph}(x, b)$  and  $a_{ms}(x, b)$  are illustrated in Fig. 1. The behaviour of the photon and marginally bound and stable orbits for the extreme black holes with  $0 \leq b \leq 1$  is illustrated in Fig. 2.

<sup>3</sup> The upper sign in (22) and (23) is relevant for the black hole spacetimes, while both signs are relevant for the naked singularity spacetimes.

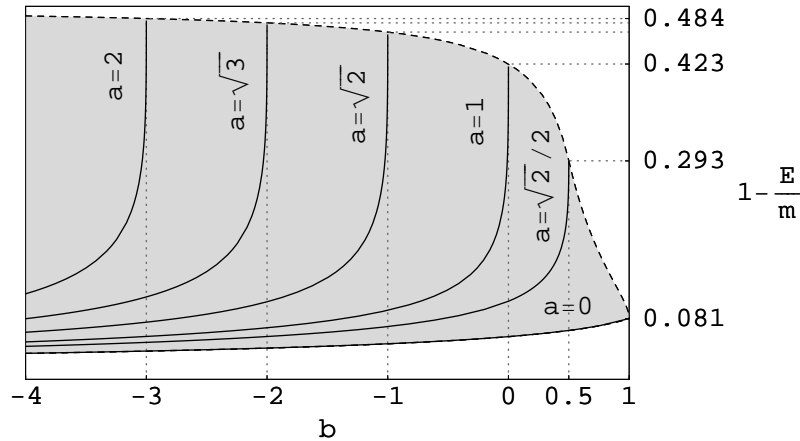


**Fig. 3** The specific binding energy per unit mass ( $E_b = 1 - E(x = x_{\text{ms}})/m$ ) of a particle at the marginally stable direct orbit  $x = x_{\text{ms}}$  as a function of the brany parameter  $b$ . The binding energy profile in thin Keplerian disc is given for appropriately chosen values of black hole spin  $a$  (full lines). The dashed line corresponds to the binding energy for maximally rotating (extreme) braneworld black holes. We can see that for extreme black hole with  $b = -3$  and  $a = 2$  the specific binding energy  $E_b \simeq 48.4\%$ , while for extreme Kerr black hole with  $b = 0$ ,  $a = 1$  we have  $E_b \simeq 42.3\%$  and for extreme case of the Reissner–Nordström black hole where  $b = 1$  and  $a = 0$  there is  $E_b \simeq 8.1\%$ . So for the class of corotating orbits, the negative tidal charge tends to increase the efficiency of an accretion disc around a maximally rotating braneworld black hole.

It is evident (see Fig. 1) that the positive tidal charge will play the same role in its effect on the circular orbits as the electric charge in the Kerr–Newman spacetime – the radius of the circular photon orbit, as well as the radii of the innermost bound and the innermost stable circular orbits move towards the event horizon as the positive tidal charge increases for both direct and retrograde orbits. For the negative tidal charge the distance of the radii of the limiting photon orbit, the innermost bound and the innermost stable circular orbits from the event horizon enlarge as the absolute value of  $b$  increases for both direct and retrograde motions of the particles [8]. Further, for the class of direct orbits, the negative tidal charge tends to increase the efficiency of accretion processes in accretion disc around a maximally rotating braneworld black hole (the specific binding energy of a particle at the marginally stable direct orbit is given for appropriately chosen values of  $a$  in Fig. 3 [8]). The specific binding energy, i.e.,  $E_b = 1 - E(x = x_{\text{ms}}, a, b)$ , decreases with descending brany parameter  $b$  with spin  $a$  being fixed; its maximum is reached when  $b$  gives the extreme black hole (Fig. 3). On the other hand, the binding energy of extreme black holes grows with descending brany parameter  $b$ . For example, for  $b = 1$  ( $a = 0$ )  $E_b = 0.081$ , for  $b = 0.5$  ( $a = \sqrt{2}/2$ )  $E_b = 0.293$ , for  $b = 0$  ( $a = 1$ )  $E_b = 0.423$ , for  $b = -1$  ( $a = \sqrt{2}$ )  $E_b = 0.465$ , for  $b = -3$  ( $a = 2$ )  $E_b = 0.484$ .

#### 4 Epicyclic oscillations of Keplerian motion

It is well known that for oscillations of both thin Keplerian [39,43] and toroidal discs [62] around black holes (neutron stars) the orbital Keplerian frequency  $\nu_K$  and the related radial and vertical epicyclic frequencies  $\nu_r$  and  $\nu_\theta$  of geodetical quasircular motion are relevant and observable directly or through some combinational frequencies [80,83,84,71]. Of course, for extended tori, the eigenfrequencies of their oscillations are shifted from the epicyclic frequencies in dependence on the thickness of the torus [68,16]. Similarly, due to non-linear resonant phenomena, the oscillatory eigenfrequencies could be shifted from the values corresponding to the geodetical epicyclic frequencies in dependence on the oscillatory amplitude [47]. It is expected that shift of this kind is observed in neutron star systems [1,2], while in microquasars, i.e., binary black hole systems, the observed frequency scatter is negligible and the geodetical epicyclic frequencies should be relevant. Here, we restrict our attention to the geodetical epicyclic oscillations of Keplerian discs in microquasars. Such an approach is quite correct for efficiently radiating discs [58] in high accretion rates. However, in low accretion rates the accretion discs radiate inefficiently, and due to the pressure effects they become thick in the innermost part being advection dominated (so called ADAFs [56,3]). The eigenfrequencies of oscillations of such toroidal structures deviate from the geodetical epicyclic frequencies up to 20% for relative high thickness of



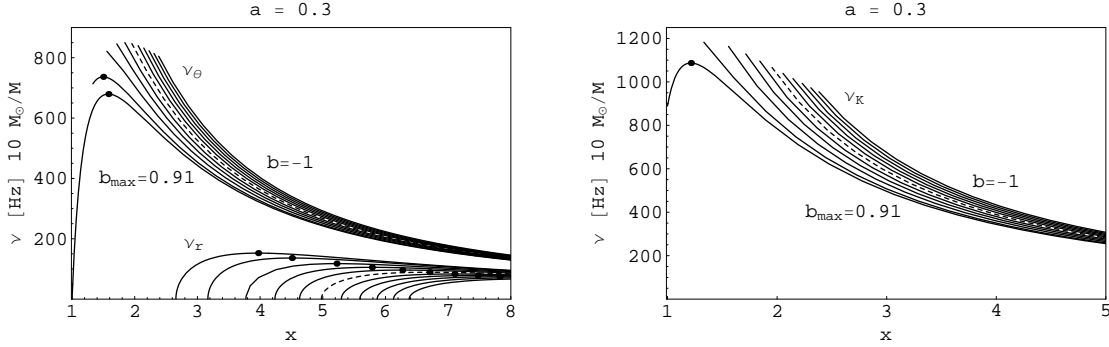


**Fig. 4** The behaviour of the two epicyclic frequencies  $\nu_r$ ,  $\nu_\theta$  (left panel), and Keplerian frequency  $\nu_K$  (right panel) in the field of braneworld Kerr black holes with fixed value of the black hole spin  $a = 0.3$  and various values of the tidal charge parameter  $b$ . The curves are spaced by 0.2 in  $b$  and they are plotted from the outer event black hole horizon  $x_h$ . The dashed lines represent Kerr spacetime with zero tidal charge.

the tori, in realistic disc configurations it is expected to be  $< 10\%$  [68, 16]. Note that the epicyclic oscillatory frequencies could be also efficiently influenced by the strong magnetic field of neutron stars, as shown in [14]. Of course, no strong magnetic field can be related to black holes [54].

In the case of the Kerr black holes with the brany tidal charge  $b$ , the formulae of the test particle geodetical circular motion and its epicyclic oscillations, obtained by Aliev and Galtsov [6], could be directly applied. We can write down the following relations for the orbital and epicyclic frequencies:

$$v_r^2 = \alpha_r v_K^2, \quad (28)$$

$$v_\theta^2 = \alpha_\theta v_K^2, \quad (29)$$

where the Keplerian frequency reads

$$v_K = \frac{1}{2\pi} \left( \frac{GM}{r_G^3} \right)^{1/2} \frac{\sqrt{x-b}}{x^2 + a\sqrt{x-b}} = \frac{1}{2\pi} \frac{c^3}{GM} \frac{\sqrt{x-b}}{x^2 + a\sqrt{x-b}}, \quad (30)$$

and the dimensionless quantities determining the epicyclic frequencies are given by

$$\alpha_r(x, a, b) = \frac{4(b-x-a^2)}{x^2} + \frac{8a\sqrt{x-b}}{x^2} + \frac{x(x-2)+a^2+b}{x(x-b)}, \quad (31)$$

$$\alpha_\theta(x, a, b) = 1 + \frac{2a^2}{x^2} - \frac{2a\sqrt{x-b}}{x^2} - \frac{2a\sqrt{x-b}}{x(x-b)} + \frac{a^2}{x(x-b)}, \quad (32)$$

which reduce to the standard relations for quasicircular geodesics in Kerr metric [84] for  $b = 0$ .

In the limit of the Reissner–Nordström like static braneworld black hole ( $a = 0$ ), we arrive at

$$\alpha_r(x, b) = \frac{4(b-x)}{x^2} + \frac{x(x-2)+b}{x(x-b)}, \quad (33)$$

$$\alpha_\theta(x, b) = 1, \quad (34)$$

so that  $v_K(x, b) = v_\theta(x, b)$  due to the spherical symmetry of the spacetime.

In the field of brany Kerr black holes ( $a \neq 0$ ), there is (see Fig. 4)

$$v_K(x, a, b) > v_\theta(x, a, b) > v_r(x, a, b), \quad (35)$$

however, this statement is not generally correct in the case of brany Kerr naked singularities. In the next section we show that the case  $v_\theta(x, a, b) \leq v_r(x, a, b)$  is also possible.

The properties of  $v_K$ ,  $v_\theta$ ,  $v_r$  for Kerr black hole spacetimes are reviewed, e.g., in [39] and for both Kerr black hole and Kerr naked singularity spacetimes in [84]. We can summarize that in Kerr spacetime with zero tidal charge ( $b = 0$ )

- the Keplerian frequency is a monotonically decreasing function of radius for the whole range of black hole rotational parameter  $a \in (-1, 1)$  in astrophysically relevant radii above the photon circular orbit;
- for slowly rotating black holes the vertical epicyclic frequency is a monotonically decreasing function of radius in the same radial range as well; however, for rapidly rotating black holes this function has a maximum;
- the radial epicyclic frequency has a local maximum for all  $a \in (-1, 1)$ , and vanishes at the innermost stable circular geodesic;
- for Kerr naked singularities the behaviour of the epicyclic frequencies is different; a detailed analysis [84] shows that the vertical frequency can have two local extrema, and the radial one even three local extrema.

In the next section we discuss the behaviour of the fundamental orbital frequencies for Keplerian motion in the field of both brany Kerr black holes and brany Kerr naked singularities.

We express the frequency as  $\nu$  [Hz]  $10M_{\odot}/M$  in every quantitative plot of frequency dependence on radial coordinate  $x$ , i.e., displayed value is the frequency relevant for a central object with a mass of  $10M_{\odot}$ , which could be simply rescaled for another mass by just dividing the displayed value by the respective mass in units of ten solar mass.

## 5 Properties of the Keplerian and epicyclic frequencies

First, it is important to find the range of relevance for the functions  $\nu_K(x, a, b)$ ,  $\nu_{\theta}(x, a, b)$ ,  $\nu_r(x, a, b)$  above the event horizon  $x_h$  for black holes, and above the ring singularity located at  $x = 0$  ( $\theta = \pi/2$ ) for naked singularities.

Stable circular geodesics, relevant for the Keplerian, thin accretion discs exist for  $x > x_{ms}(a, b)$ , where  $x_{ms}(a, b)$  denotes the radius of the marginally stable orbit, determined (in an implicit form) by the relation (23), which coincides with the condition

$$\alpha_r(x, a, b) = 0. \quad (36)$$

For toroidal, thick accretion discs the unstable circular geodesics can be relevant in the range  $x_{mb} \leq x_{in} < x < x_{ms}$ , being stabilized by pressure gradients in the tori. The radius of the marginally bound circular geodesic  $x_{mb}$ , implicitly determined by the equation (22), is the lower limit for the inner edge of thick discs [44, 45].

Clearly, the Keplerian orbital frequency is well defined up to  $x = x_{ph}$ . However,  $\nu_r$  is well defined, if  $\alpha_r \geq 0$ , i.e., at  $x \geq x_{ms}$ , and  $\nu_r = 0$  at  $x_{ms}$ . We can also show that for  $x \geq x_{ph}$ , there is  $\alpha_{\theta} \geq 0$ ; i.e., the vertical frequency  $\nu_{\theta}$  is well defined at  $x > x_{ph}$ .

From Fig. 4, we can conclude that not only the both epicyclic frequencies but even the Keplerian frequency can have a maximum located above the outer event black hole horizon; this kind of behaviour is not allowed in the Kerr spacetimes. In the next subsection we will discuss, if the maximum of  $\nu_K(x, a, b)$  could be located above the marginally stable or the limiting photon circular orbit.

### 5.1 Local extrema of the Keplerian frequency

Denoting by  $\mathcal{X}_K$  the local extrema of the Keplerian frequency  $\nu_K$ , we can give the extrema by the condition

$$\frac{\partial \nu_K}{\partial x} = 0. \quad (37)$$

From (30), we find that the corresponding derivative<sup>4</sup> is

$$\nu'_K = \frac{1}{2\pi} \sqrt{\frac{GM}{r_G^3}} \frac{x(4b - 3x)}{2\sqrt{x-b}(x^2 + a\sqrt{x-b})^2} = \frac{x(4b - 3x)\nu_K}{2(x-b)(x^2 + a\sqrt{x-b})}, \quad (38)$$

and relation (37) implies that the Keplerian frequency has a local extremum located at

$$\mathcal{X}_K = \frac{4}{3}b. \quad (39)$$

<sup>4</sup> After introducing ' as d/dx.

The second derivative at  $x = \mathcal{X}_K$

$$v_K'' = -\frac{1}{2\pi} \sqrt{\frac{GM}{r_G^3}} \frac{162\sqrt{3}}{\sqrt{b}(3\sqrt{3}a + 16b^{3/2})^2} \quad (40)$$

is always negative, thus the Keplerian frequency has a local maximum at  $x = \mathcal{X}_K$ , independently of the spin parameter  $a$ .

Generally, the maximum is located at or above the outer event black hole horizon if the condition

$$\mathcal{X}_K \geq 1 \quad (41)$$

is satisfied that implies the relevant range of the tidal charge parameter

$$0.75 \leq b \leq 1 \quad (42)$$

and from relation (24) we conclude that the possible values of the black hole spin are allowed at the interval

$$0 \leq a \leq 0.5. \quad (43)$$

The case of  $a = 0.5$  and  $b = 0.75$  corresponds to the maximally rotating (extreme) braneworld Kerr black hole.

From relations (20) and (21) we obtain

$$a_h(x = \mathcal{X}_K) = \frac{1}{3} \sqrt{b(15 - 16b)}, \quad (44)$$

$$a_{ph}(x = \mathcal{X}_K) = \sqrt{3b} \left(1 - \frac{8}{9}b\right), \quad (45)$$

which implicitly determine that the maximum of the Keplerian frequency radial profile is situated at the radius coinciding with the radius of the black hole horizon  $\mathcal{X}_K = x_h$  (44) or the circular photon orbit  $\mathcal{X}_K = x_{ph}$  (45).

The functions  $a_h(x = \mathcal{X}_K)$ ,  $a_{ph}(x = \mathcal{X}_K)$  are shown in the left panel of Fig. 5. We can see that for brany Kerr black holes all possible values of the tidal charge parameter and black hole spin imply the condition

$$a_{ph}(x = \mathcal{X}_K) \geq a_{max}, \quad (46)$$

thus the maximum of the Keplerian frequency could never be located above the photon orbit  $x_{ph}$  (and the marginally stable orbit  $x_{ms}$ ). Only for maximally rotating black hole with  $b = 0.75$  and  $a = a_{max} = 0.5$ , the maximum is situated exactly at the Boyer–Lindquist coordinate radius of the limiting photon orbit that merges with the radius of the black hole horizon, so  $\mathcal{X}_K = x_{ph} = x_h = 1$  (see Fig. 6).<sup>5</sup>

We can conclude that for brany parameter from interval (42) and black hole spin from interval (43), the Keplerian frequency has its maximum located between the black hole horizon and the photon circular orbit

$$x_h \leq \mathcal{X}_K \leq x_{ph}. \quad (47)$$

Clearly, the maximum of the Keplerian frequency is physically irrelevant for all the brany Kerr black holes. In astrophysically relevant radii above the photon orbit,  $x > x_{ph}$ , the Keplerian frequency is a monotonically decreasing function of radius for the whole range of the brany tidal charge parameter  $b$ , as in the standard Kerr spacetimes. In the brany Kerr naked singularity spacetimes, the situation is more complicated, because of the complexity of the behaviour of the functions  $a_{ph}(x, b)$  and  $a_{ms}(x, b)$ . The situation is clearly illustrated in Fig. 5.

---

<sup>5</sup> However, note the behaviour of extreme Kerr black hole at  $x = 1$ , where the same coordinate corresponds to an infinitely long throat of the proper radial distance, with different positions of the horizon and the circular photon, marginally bound and marginally stable orbits [15].

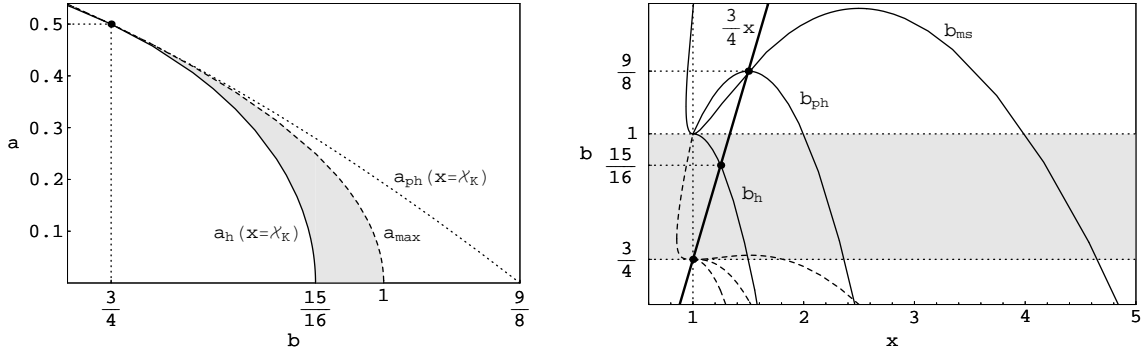


**Fig. 5** *Left panel*: the functions  $a_h(x = \mathcal{X}_K)$  (solid line),  $a_{ph}(x = \mathcal{X}_K)$  (dotted line) determining that the maximum of the Keplerian frequency is situated exactly at the black hole horizon radius  $\mathcal{X}_K = x_h$ , or at the photon orbit  $\mathcal{X}_K = x_{ph}$ . Dashed line represents maximum possible value of the black hole spin corresponding to the concrete value of the brany parameter  $b$ , so the area above  $a_{max}$  belongs to naked singularities. The gray area illustrates all possible combinations of the black hole spin  $a$  and the tidal charge  $b$  for which the Keplerian frequency has its maximum located at  $x_h \leq \mathcal{X}_K \leq x_{ph}$ . The *right panel* displays the functions  $b_h$ ,  $b_{ph}$  and  $b_{ms}$  implicitly determining the location of the black hole horizon, the limiting photon orbit and the marginally stable orbit for  $a = 0$  (solid lines) and  $a = 0.5$  (dashed lines). Thick line represents the maximum of the Keplerian frequency  $b = 3x/4$ .

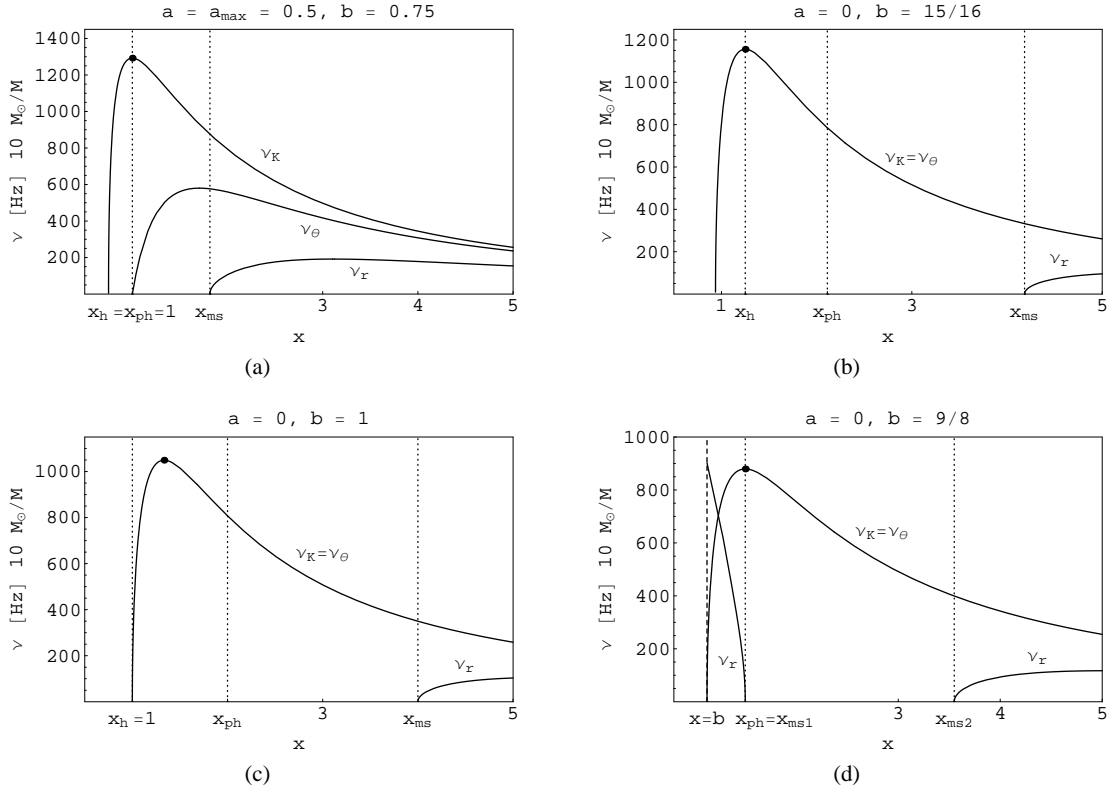


**Fig. 6** The Keplerian and epicyclic frequencies for various values of the black hole spin  $a$  and the tidal charge  $b$ : (a) the only case when the Keplerian frequency has its maximum located exactly at  $\mathcal{X}_K = x_h = x_{ph}$ ; (b)–(d) represent braneworld Reissner–Nordström spacetime where  $\nu_K = \nu_\theta$ ; (a), (c) correspond to the extreme black holes, (d) to a naked singularity spacetime (notice that the condition  $x > b$  has to be satisfied).

## 5.2 Local extrema of epicyclic frequencies

It is important to determine for a given spacetime (with parameters  $a$  and  $b$ ), if profiles of both the epicyclic frequencies have a local extrema in the region of relevance ( $x > x_{\text{ms}}(a, b)$ ), since in such a case the resonant radii might not be given uniquely (i.e., the same frequency ratio can appear at different resonant radii, with different frequencies), and the analysis of resonant phenomena must then be done very carefully [84].

The local extrema of the radial and vertical epicyclic frequencies  $\mathcal{X}_r$ ,  $\mathcal{X}_\theta$  are given by the condition

$$\frac{\partial v_i}{\partial x} = 0 \quad \text{for } \mathcal{X}_i, \quad \text{where } i \in \{r, \theta\}. \quad (48)$$

Using (28) and (29), the corresponding derivatives can be given in the form

$$v'_i = \sqrt{\alpha_i} \left( v'_K + \frac{\alpha'_i}{2\alpha_i} v_K \right), \quad (49)$$

$$\alpha'_i = \frac{\beta_i}{x^3(x-b)^{5/2}}, \quad (50)$$

where  $v'_K$  is given by (38), and

$$\begin{aligned} \beta_r(x, a, b) &= -4a(3x-4b)(x-b)^2 \\ &\quad + \sqrt{x-b} [a^2(6x^2-15xb+8b^2) - (x^3b-6x^3+18x^2b-21xb^2+8b^3)], \end{aligned} \quad (51)$$

$$\beta_\theta(x, a, b) = a \left( x - a\sqrt{x-b} - b \right) (6x^2 - 9xb + 4b^2). \quad (52)$$

Relations (48) and (49) imply the condition determining extrema  $\mathcal{X}_i(a, b)$  of the epicyclic frequency profiles

$$\beta_i(x, a, b) = -\frac{2v'_K}{v_K} x^3(x-b)^{5/2} \alpha_i(x, a, b), \quad i \in \{r, \theta\}. \quad (53)$$

We have checked that in the case of counterrotating orbits ( $a < 0$ ) the extrema  $\mathcal{X}_\theta$  are located under the photon circular orbit and the extrema  $\mathcal{X}_r$  are just extensions of the  $\mathcal{X}_r$  for corotating case. Therefore, we focus on the case of corotating orbits ( $a > 0$ ) in the next discussion.

In Fig. 7 (8) we show for various values of brany parameter  $b$  curves  $\mathcal{A}_r^k(x = \mathcal{X}_r, b)$  ( $\mathcal{A}_\theta^k(x = \mathcal{X}_\theta, b)$ ),  $k \in \{1, 2\}$  implicitly determined by the relations (53); index  $k$  denotes different branches of the solution of (53).

The marginally stable orbit radius  $x_{\text{ms}}$  (where  $\alpha_r = 0$ ) falls with tidal charge  $b$  growing and spin  $a$  being fixed.

### 5.2.1 Radial epicyclic frequency

For all possible values of the brany parameter  $b$ , the radial epicyclic frequency  $v_r$  has one local maximum for braneworld Kerr black holes with rotational parameter restricted by

$$0 \leq a \leq a_{\text{max}}(b). \quad (54)$$

The local maximum is always located above the marginally stable orbit  $x_{\text{ms}}$  (see Fig. 7).

In the case of naked singularities, the situation is complicated and the discussion can be separated into three parts according to the parameter  $b$ .

(a)  $b < b_c \doteq 0.29143$

In the field of such brany Kerr naked singularities the radial epicyclic frequency has two local maxima and one local minimum for

$$a_{\text{max}} < a < a_{\text{c1}(r)}, \quad (55)$$

where  $a_{\text{c1}(r)}$  corresponds to the local maximum of  $\mathcal{A}_r^1(x = \mathcal{X}_r, b)$ , and one local maximum for

$$a \geq a_{\text{c1}(r)}, \quad (56)$$

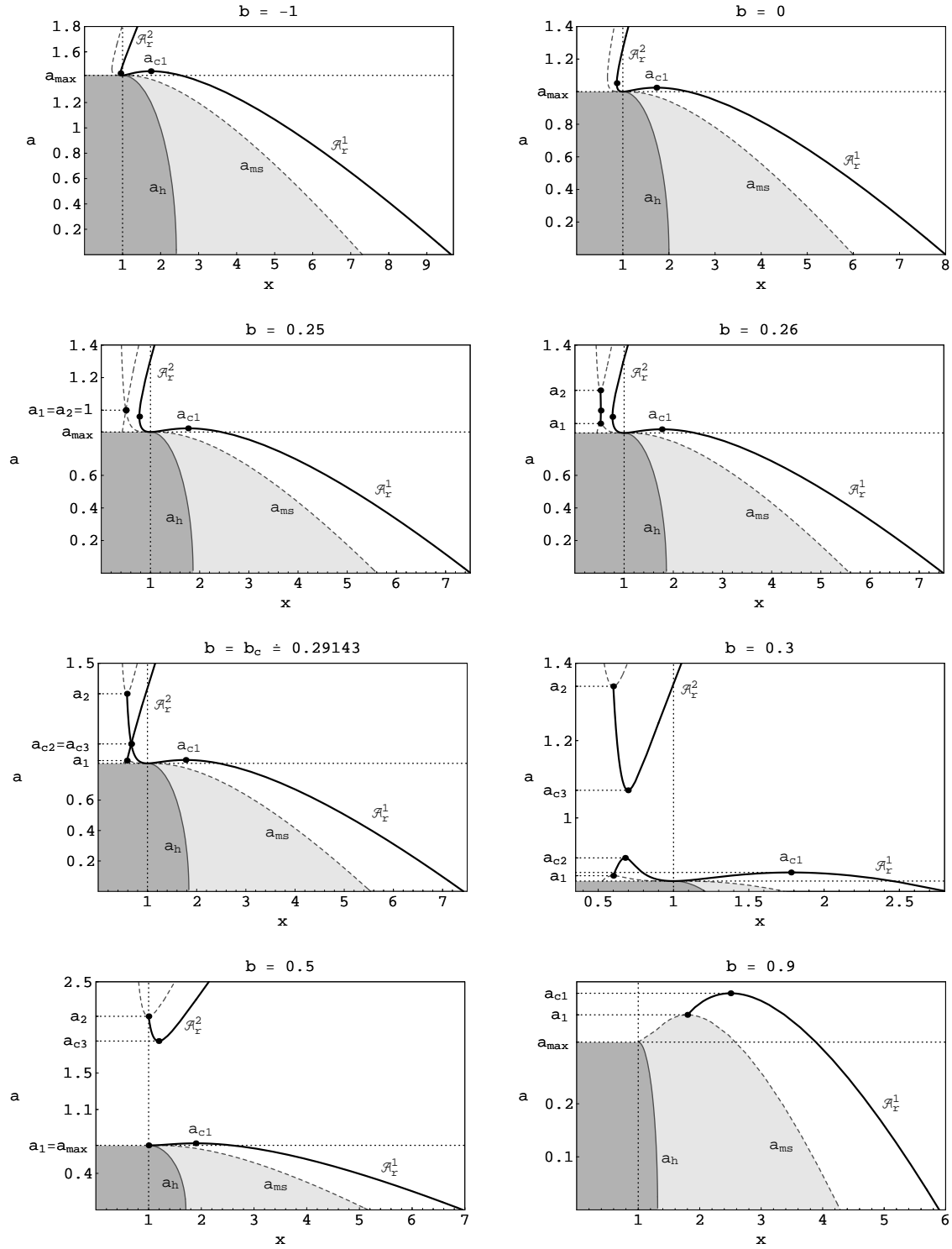


**Fig. 7** The functions  $\mathcal{A}_r^1(x = \mathcal{X}_r, b)$ ,  $\mathcal{A}_r^2(x = \mathcal{X}_r, b)$ , implicitly determining the locations  $\mathcal{X}_r$  of the radial epicyclic frequency local extrema for various values of brany parameter  $b$ .

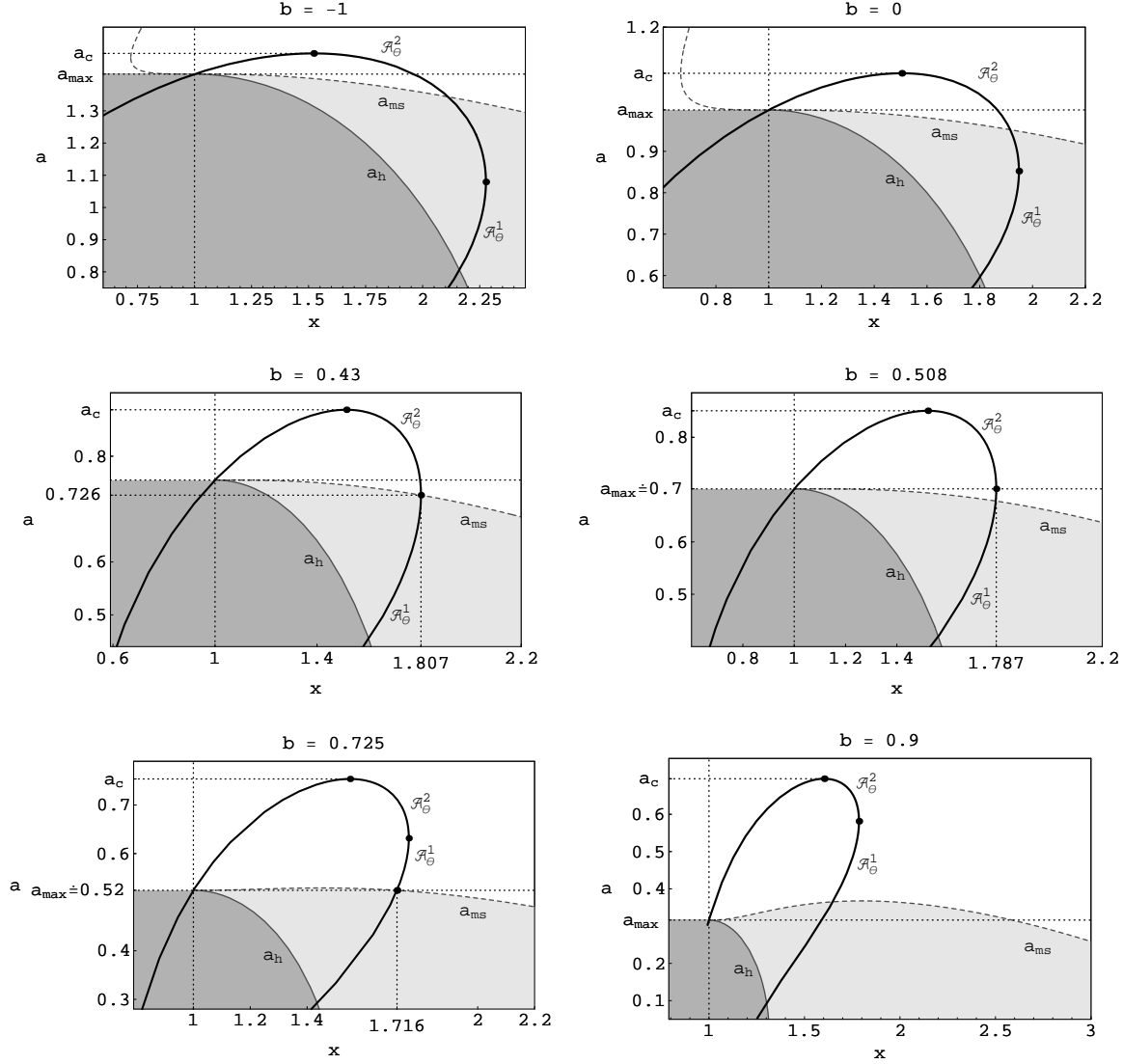


**Fig. 8** The functions  $\mathcal{A}_\theta^1(x = \mathcal{X}_\theta, b)$ ,  $\mathcal{A}_\theta^2(x = \mathcal{X}_\theta, b)$ , implicitly determining the locations  $\mathcal{X}_\theta$  of the vertical epicyclic frequency local extrema for typical values of the brany parameter  $b$ .

as usual in Kerr naked singularity spacetimes [84]. However, for values of spin  $a$  satisfying the condition

$$a_1 < a < a_2, \quad (57)$$

where  $a_1$  is given by the equation

$$\mathcal{A}_r^1(x = \mathcal{X}_r, b) = a_{ms} \quad (58)$$

and  $a_2$  is given by

$$\mathcal{A}_r^2(x = \mathcal{X}_r, b) = a_{ms}, \quad (59)$$

the radial epicyclic frequency has one extra local minimum, because in brany Kerr naked singularity spacetimes with these special values of  $a$  there exists no marginally stable orbit (as given by the condition (36), i.e.,  $v_r = 0$ ). Therefore, at  $x > 0$  the radial epicyclic frequency is for  $a$  from the interval (57) always greater than zero.

For braneworld Kerr naked singularities with  $b > b_c$ , the situation is even more complicated, as we can see in Fig. 7. We denote  $a_{c1(r)}$  and  $a_{c2(r)}$  the local maxima of  $\mathcal{A}_r^1(x = \mathcal{X}_r, b)$ , and  $a_{c3(r)}$  the local minimum of  $\mathcal{A}_r^2(x = \mathcal{X}_r, b)$ .

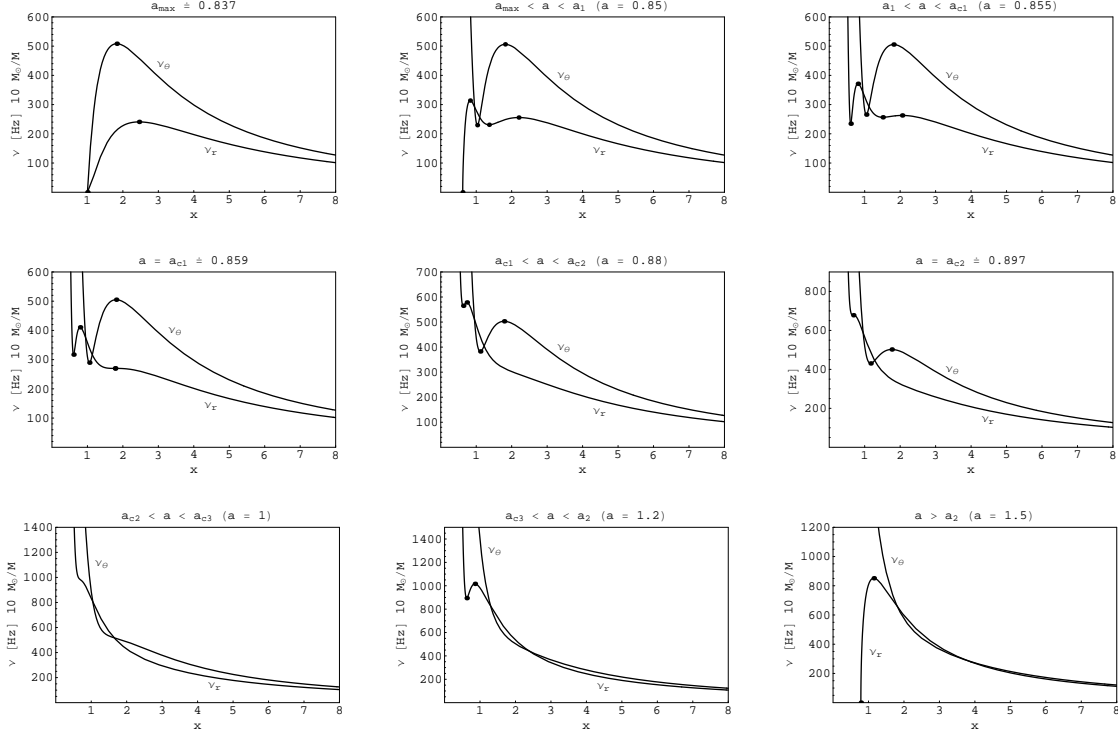


**Fig. 9** The behaviour of the epicyclic frequencies for  $b = 0.3$  and for some representative values of rotational parameter  $a$  in braneworld Kerr naked singularity spacetimes. For comparison, an extreme braneworld Kerr black hole case is included.

(b)  $b_c < b < 0.5$

In such a case, we consider two possible relations of the spin parameter, namely  $a_{c2(r)} > a_{c1(r)}$  (or  $a_{c2(r)} < a_{c1(r)}$ ). Then we find that the radial epicyclic frequency has for  $a_{\max} < a \leq a_1$  two local maxima and one local minimum, for  $a_1 < a < a_{c1(r)}$  ( $a_1 < a < a_{c2(r)}$ ) two local maxima and also two local minima, for  $a_{c1(r)} \leq a < a_{c2(r)}$  ( $a_{c2(r)} \leq a < a_{c1(r)}$ ) one local maximum and one local minimum, for  $a_{c2(r)} \leq a \leq a_{c3(r)}$  ( $a_{c1(r)} \leq a \leq a_{c3(r)}$ ) the radial epicyclic frequency is a monotonically decreasing function of the radial coordinate without any extrema, for  $a_{c3(r)} < a < a_2$  it has again one local maximum and one local minimum, and finally for  $a \geq a_2$  it has only one local maximum as in the black hole spacetimes ( $a_1$  and  $a_2$  are given by (58) and (59), the condition  $a_{\max} < a_1 < a_{c1(r)}$  is always satisfied). Notice that for  $a_1 < a < a_2$ ,  $\nu_r$  could not be equal to zero (see Fig. 9).

For  $b = 0.5$ , there is  $a_1 = a_{c2(r)} = a_{\max} = \sqrt{2}/2$ , and for  $a_{\max} < a < a_{c1(r)}$  the radial epicyclic frequency has one local maximum and one local minimum, for  $a_{c1(r)} \leq a \leq a_{c3(r)}$  it is a monotonically decreasing function of the radial coordinate without any extrema, for  $a_{c3(r)} < a < a_2$  it has again one local maximum and one local minimum, and for  $a \geq a_2$  it has only one local maximum.

(c)  $b > 0.5$

In the case of braneworld Kerr naked singularities with such brany parameters the behaviour of the radial epicyclic frequency is different due to the effect related to the loci of the marginally stable orbits as described in Section 3 (see relation (27)). For  $a_{\max} < a \leq a_1$ ,  $\nu_r$  has one local maximum, for  $a_1 < a < a_{c1(r)}$  it has one local maximum and one local minimum, for  $a_{c1(r)} \leq a \leq a_{c3(r)}$  it is a monotonically decreasing function of the radial coordinate without any extrema, for  $a_{c3(r)} < a < a_2$  it has again one local maximum and one local minimum, and finally for  $a \geq a_2$  it has only one local maximum.

### 5.2.2 Vertical epicyclic frequency

Qualitatively different types of its behaviour in dependence on the brany parameter  $b$  are illustrated in Fig. 8.



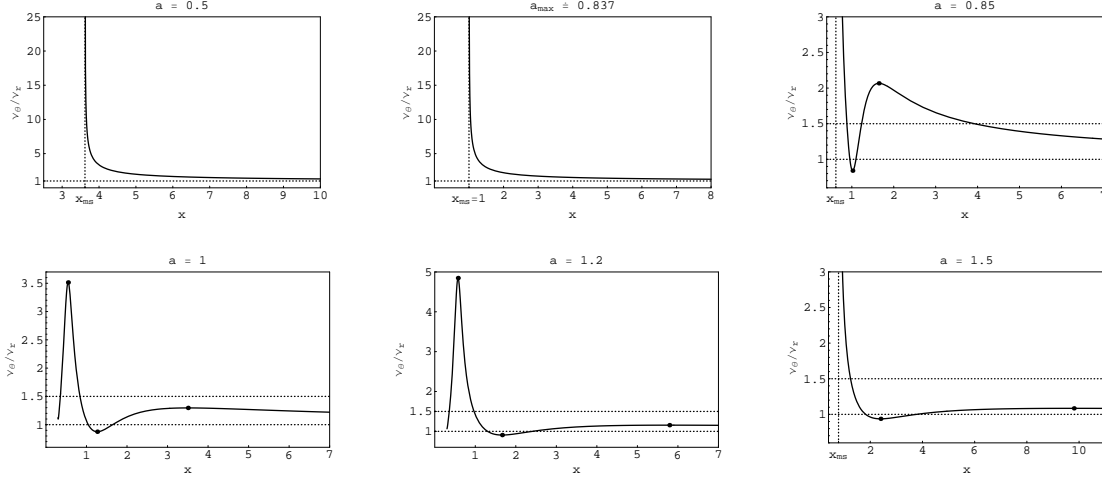


**Fig. 10** The behaviour of ratio  $v_\theta/v_r(x)$  of the epicyclic frequencies for braneworld Kerr black hole and naked singularity spacetimes with  $b = 0.3$ . The marginally stable orbit  $x_{\text{ms}}$  is denoted by a dotted vertical line (if this orbit exists at the given spacetime).

The vertical epicyclic frequency has a local maximum (at  $x > x_{\text{ms}}$ ) only for rapidly rotating black holes with (see Fig. 8)

$$a_{\text{ms}}(\theta) < a < a_{\text{max}} \quad \text{and} \quad b < 0.725, \quad (60)$$

where  $a_{\text{ms}}(\theta)$  is the solution of the equation

$$a_{\text{ms}} = \mathcal{A}_\theta^k, \quad (61)$$

for  $k = 1$  or  $2$ . There is  $a_{\text{ms}}(\theta) = a_{\text{max}}(b = 0.725) \doteq 0.524$ . (For maximally rotating black hole with  $b = 0.725$  and  $a_{\text{max}} \doteq 0.524$ , the local maximum is located exactly at the radius of the marginally stable orbit,  $\mathcal{X}_\theta = x_{\text{ms}}$ ). Recall that in the black hole case the local maximum of  $v_\theta(x, a, b)$  is relevant in resonant effects at  $x > x_{\text{ms}}$ . For  $b > 0.725$  the vertical epicyclic frequency is a monotonically decreasing function of radius for the whole range of black hole rotational parameter  $a$ .

In the braneworld Kerr naked singularity spacetimes, the function  $v_\theta$  has a local minimum and a local maximum for

$$a_{\text{max}} < a < a_{\text{c}}(\theta), \quad (62)$$

and has no astrophysically relevant local extrema for

$$a \geq a_{\text{c}}(\theta). \quad (63)$$

We can summarize that for braneworld black holes with any value of  $b$  the radial epicyclic frequency profile has a local maximum and zero point at  $x = x_{\text{ms}}$ , as in the case of standard Kerr black holes. The vertical epicyclic frequency has a local maximum for spin  $a$  close to extreme black hole states for values of  $b < 0.725$  as in the standard Kerr case, but it is purely monotonically decreasing function of radius for black holes with  $b \geq 0.725$ .

The behaviour of the epicyclic frequencies substantially differs for braneworld Kerr naked singularities in comparison with braneworld Kerr black holes. Examples of the behaviour of the epicyclic frequencies in Kerr naked singularity spacetimes with  $b = 0.3$  are given in Fig. 9.

### 5.3 Ratio of epicyclic frequencies

The ratio of epicyclic frequencies  $v_\theta$  and  $v_r$  is crucial for the orbital resonance models of QPOs [5, 37]. It is well known [39, 84] that for the Kerr black holes ( $-1 \leq a \leq 1$ ) the inequality

$$v_r(x, a) < v_\theta(x, a) \quad (64)$$

holds, i.e., the equation  $v_r(x, a) = v_\theta(x, a)$  does not have any real solution in the whole range of black hole rotational parameter  $a \in (-1, 1)$  and

$$\frac{v_\theta}{v_r} > 1 \quad (65)$$

for any Kerr black hole. Furthermore, this ratio is a monotonic function of radius for any fixed  $a \in (-1, 1)$  [84]. These statements are valid also for any brany Kerr black hole (i.e., for  $b$  fixed and  $a \leq a_{\max}$ ).

However, the situation is different for Kerr naked singularities. For  $b = 0$  and  $a > 1$ , the epicyclic frequencies  $v_\theta$ ,  $v_r$  can satisfy the equality condition

$$v_\theta(a, x) = v_r(a, x) \quad (66)$$

giving a possibility of strong resonant phenomenon, which could occur at the critical radius

$$x_{\text{sr}} = a^2 \quad (a \geq 1). \quad (67)$$

This means that for any Kerr naked singularity the epicyclic frequency ratio  $v_\theta/v_r$  is a non-monotonic function that reaches value 1 at the point given by (67) [84].

Furthermore, for brany Kerr naked singularities with  $b > 0$  the epicyclic frequencies can satisfy even the condition (see Figs 9 and 10)

$$v_\theta(x, a, b) \leq v_r(x, a, b), \quad (68)$$

that is not allowed in Kerr naked singularities. For naked singularities with  $b < 0$  the relation

$$v_\theta(x, a, b) > v_r(x, a, b) \quad (69)$$

is valid, as in the Kerr black hole spacetimes.

#### 5.4 Ratio of Keplerian and epicyclic frequencies

We have to consider the possibility of  $v_K < v_r(v_\theta)$ , since such a situation could imply change in the maximum frequency supposed to be given by  $v_K$  at  $x_{\text{ms}}$ , observable in the field of a black hole (or a naked singularity). We have to look for the possibility to satisfy the condition  $v_K = v_r(v_\theta)$  (i.e.,  $\alpha_r(\alpha_\theta) = 1$ ).

For the radial epicyclic frequency we arrive to the condition

$$a = a_{\text{sr}}^r(x, b) \equiv \frac{4(x-b)^{3/2} \pm x\sqrt{(3-4b)b + (3b-2)x}}{3x-4b}. \quad (70)$$

For the vertical epicyclic frequency there are two solutions of the equation  $\alpha_\theta = 1$ , the first one reads

$$a = a_{\text{sr}}^\theta(x, b) \equiv \frac{2(2x-b)\sqrt{x-b}}{3x-2b} \quad (71)$$

and the second one is  $a = 0$ , representing the Reissner–Nordström braneworld solution, where  $v_\theta = v_K$  due to the spherical symmetry of the spacetime.

The relations (70) and (71) are illustrated in Fig. 11. We can see that

$$a_{\text{sr}}^r(x, b) > a_{\max} \quad \text{and} \quad a_{\text{sr}}^\theta(x, b) > a_{\max}, \quad (72)$$

so we can conclude that for braneworld black holes the condition

$$v_K > v_\theta > v_r \quad (73)$$

is satisfied, similarly to the case of standard Kerr black holes. On the other hand, in brany Kerr naked singularity spacetimes, the epicyclic frequencies could overcome the Keplerian frequency at small radii (see Fig. 6(d)). We not go into detailed discussion since we concentrate on the black hole case.

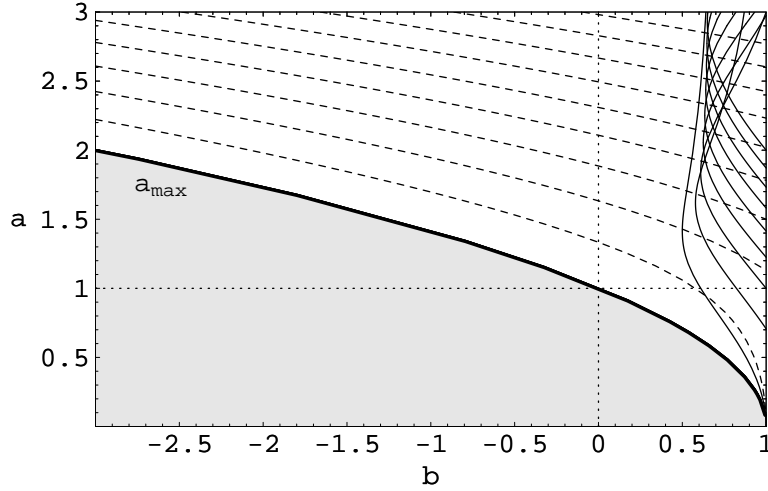


**Fig. 11** The functions  $a_{\text{sr}}^r(x, b)$  (solid lines) and  $a_{\text{sr}}^\theta(x, b)$  (dashed lines) that represent the values of the black hole spin  $a$  and the brany parameter  $b$  for which the conditions  $v_r(x, a, b) = v_K(x, a, b)$  and  $v_\theta(x, a, b) = v_K(x, a, b)$  can be satisfied. The curves are plotted for  $x = 1, 1.5, 2, 2.5, 3, 3.5, 4, 4.5, 5$ . The black thick line represents the function  $a_{\text{max}}$ , so only the gray area belongs to the black hole spacetimes. We can see that the relations  $v_\theta(x, a, b) \geq v_K(x, a, b)$  and  $v_r(x, a, b) \geq v_K(x, a, b)$  are relevant only in naked singularity spacetimes, where even the case with  $v_K(x, a, b) = v_\theta(x, a, b) = v_r(x, a, b)$  is possible (where the lines  $a_{\text{sr}}^r(x, b)$  and  $a_{\text{sr}}^\theta(x, b)$  cross each other).

## 6 Resonance conditions

The orbital resonance models for QPOs proposed in [4,5] are particularly based on resonance between oscillations with the epicyclic frequencies which are excited at a well defined resonance radius  $x_{n:m}$  given by the condition

$$\frac{v_\theta}{v_r}(a, b, x_{n:m}) = \frac{n}{m}, \quad (74)$$

where  $n:m$  is (most often) 3:2 in the case of *parametric resonance* (the effect itself is described by the Mathieu equation discussed by Landau and Lifshitz [47]) and arbitrary rational ratio of two small integral numbers (1, 2, 3, ...) in the case of *forced resonances* [5]. Another, so called “*Keplerian*” resonance model, takes into account possible parametric or forced resonances between oscillations with radial epicyclic frequency  $v_r$  and Keplerian orbital frequency  $v_K$ .

For a particular resonance  $n:m$ , the equation

$$n v_r = m v_v; \quad v_v \in \{v_\theta, v_K\} \quad (75)$$

determines the dimensionless resonance radius  $x_{n:m}$  as a function of the dimensionless spin  $a$  in the case of direct resonances that can be easily extended to the resonances with combinational frequencies [71]. From the known mass of the central black hole (e.g., low-mass in the case of binary systems or hi-mass in the case of supermassive black holes), the observed twin peak frequencies ( $v_{\text{upp}}$ ,  $v_{\text{down}}$ ), and the equations (28)–(30), (75) imply the black hole spin, consistent with different types of resonances with the beat frequencies taken into account. This procedure was first applied to the microquasar GRO 1655-40 by Abramowicz and Kluźniak [4], more recently to the other three microquasars [80] and also to the Galaxy center black hole Sgr A\* [76].

The twin peak QPOs were observed in four microquasars, namely GRO 1655-40, XTE 1550-564, H 1743-322, GRS 1915+105 [80]. In all of the four cases, the frequency ratio of the twin peaks is very close to 3:2. The very probable interpretation of observed twin peak kHz QPOs is the 3:2 parametric resonance, however, generally it is not unlikely that more than one resonance could be excited in the disc at the same time (or in different times) under different internal conditions. Indeed, observations of the kHz QPOs in the microquasar GRS 1915+105, and of the QPOs in extragalactic sources NGC 4051, MCG-6-30-15 [46] and NGC 5408 X-1 [70], and the Galaxy center Sgr A\* [13] show a variety of QPOs with frequency ratios differing from the 3:2 ratio.

The resonances could be parametric or forced and of different versions according to the epicyclic (Keplerian) frequencies entering the resonance directly, or in some combinational form. In principle, for any case

of the resonance model version, one can determine both the spin and mass of the black hole just from the eventually observed set of frequencies. However, the obvious difficulty would be to identify the right combination of resonances and its relation to the observed frequency set. Within the range of black hole mass allowed by observations, each set of twin peak frequencies puts limit on the black hole spin. Of course, the resonance model versions are consistent with observations, if the allowed spin ranges are overlapping each other. Clearly, two or more twin peaks then generally make the spin measurement more precise.

Here we consider the versions of the resonance model explaining the twin peaks with the 3:2 frequency ratio. We take into account both the direct and simple combinational resonances.

The resonant conditions determining implicitly the resonant radius  $x_{n:m}$  must be related to the radius of the innermost stable circular geodesic  $x_{\text{ms}}$  giving the inner edge of Keplerian discs. Therefore, for all the relevant resonance radii, there must be  $x_{n:m} \geq x_{\text{ms}}$ , where  $x_{\text{ms}}$  is implicitly given by (23).

First, we investigate radial coordinate where the ratio

$$\frac{v_{\text{upp}}}{v_{\text{down}}} = \frac{3}{2} \quad (76)$$

occurs for the simple case of the parametric resonance between the radial and vertical epicyclic oscillations.

The result is given in the way relating the dimensionless spin  $a$  and the dimensionless resonance radius  $x$  for frequency ratio  $n:m = 3:2$

$$a = a_{3:2}^{\theta/r}(x, b) \equiv a_{\text{EO}}(x, b) \equiv \frac{1}{39x - 44b} \left\{ 4(11x - 10b)\sqrt{x - b} - \sqrt{(5x + 4b)[39x^3 - 2x^2(17 + 22b) + 43xb - 4b^2]} \right\}. \quad (77)$$

The behaviour of the function  $a_{3:2}^{\theta/r}$  representing the direct resonance  $v_{\theta} : v_r = 3:2$  is for various values of the brany parameter  $b$  illustrated in Fig. 1. We can see that for all considered values of  $b$  the condition  $x_{3:2} > x_{\text{ms}}$  is always satisfied.

Another possibility, applied in the context of both black hole and neutron star systems producing kHz QPOs is the relativistic precession model [69]. Now, we can assume a resonance of the oscillations with the Keplerian frequency  $v_{\text{K}} \equiv v_{\text{upp}}$  and the relativistic precession frequency  $v_{\text{p}} = v_{\text{K}} - v_r \equiv v_{\text{down}}$ . Considering the condition  $v_{\text{K}} : (v_{\text{K}} - v_r) = 3:2$ , we arrive to the relation<sup>6</sup>

$$a = a_{3:2}^{\text{K}/(\text{K}-r)}(x, b) \equiv a_{\text{RP}}(x, b) \equiv \frac{12(x - b)^{3/2} - x\sqrt{6x(4x - 3) - 29xb + 27b - 4b^2}}{3(3x - 4b)}. \quad (78)$$

This is again illustrated in Fig. 1.

On the other hand, in the framework of the warp disc oscillations, the frequencies of which are given by combinations of the Keplerian and epicyclic frequencies, resonant phenomena could be relevant too. Usually, the inertial-acoustic and g-mode oscillations and their resonances are relevant [38]. Here, we give as an example the study of the simple frequency relation

$$\frac{2v_{\text{K}} - v_r}{v_{\text{K}} - v_r} = \frac{3}{2}. \quad (79)$$

However, there exists no solution for this ratio in both Kerr black hole and Kerr naked singularity spacetimes for any value of brany parameter  $b$ . The lowest relevant frequency ratio is  $(2v_{\text{K}} - v_r) : (v_{\text{K}} - v_r) = 2:1$  (see Fig. 12). Therefore, only the modification to the relation of observed frequencies [38]

$$\frac{2v_{\text{K}} - v_r}{2(v_{\text{K}} - v_r)} = \frac{3}{2} \quad (80)$$

could be relevant. Then we have

$$a = a_{3:2}^{(2\text{K}-r)/(2\text{K}-2r)}(x, b) \equiv a_{\text{TO}}(x, b) \equiv \frac{8(x - b)^{3/2} \pm x\sqrt{9x^2 - (9b + 8)x - 4(b - 3)b}}{2(3x - 4b)}. \quad (81)$$

Again, we illustrate this function in Fig. 1. For all of the tested values of the brany parameter  $b$ , the resonance radius of the trapped oscillations lies between the resonance radius of the relativistic precession oscillations and the radial and vertical epicyclic oscillations.

<sup>6</sup> Clearly, we obtain the same relation also for the direct ‘‘Keplerian’’ resonance  $v_{\text{K}} : v_r = 3:1$ .

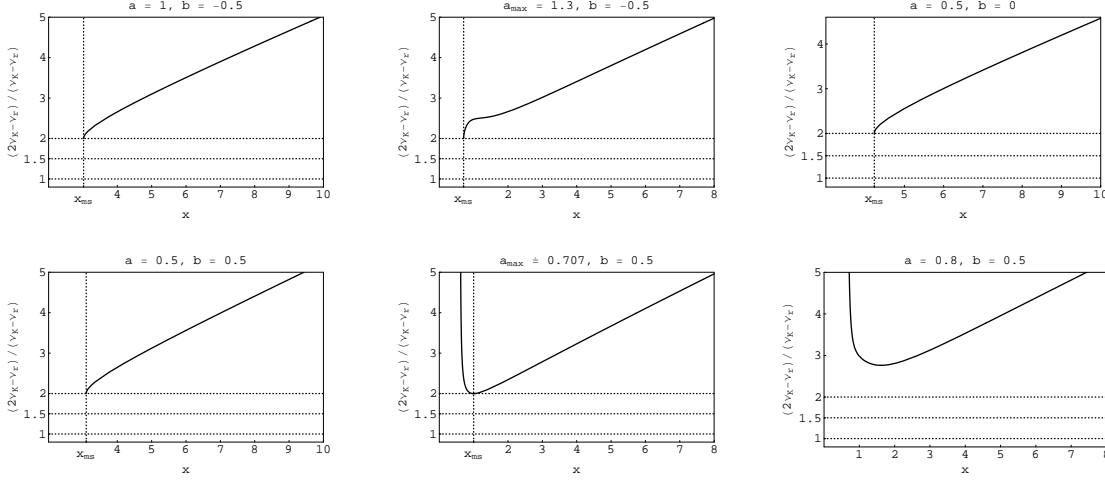


**Fig. 12** The behaviour of ratio  $(2v_K - v_r)/(v_K - v_r)$  representing the resonance of trapped oscillations assumed in warped disc [38]. The marginally stable orbit  $x_{ms}$  is denoted by a dotted vertical line (if this orbit exists at the given spacetime).

### 6.1 Application to microquasar GRS 1915+105

The frequency ratio of the upper twin peak QPOs observed in microquasar GRS 1915+105 is very close to 3:2 [80]:

$$v_{\text{upp}} = (168 \pm 3) \text{ Hz}, \quad (82)$$

$$v_{\text{down}} = (113 \pm 5) \text{ Hz}. \quad (83)$$

From the known limits on the mass of the black hole in GRS 1915+105 [51]

$$10.0M_{\odot} < M < 18.0M_{\odot}, \quad (84)$$

the observed twin peak frequencies (82), (83), and the equations (28)–(30), (75) imply the black hole spin consistent with different types of resonances. Assuming the very probable interpretation of observed twin peak kHz QPOs in microquasar as the 3:2 standard parametric resonance

$$\frac{v_{\theta}}{v_r}(a, b, x_{3:2}) = \frac{3}{2} \quad (85)$$

and identifying

$$v_{\text{upp}} \equiv v_{\theta}, \quad (86)$$

we can express the black hole mass in the form

$$M_{\text{EO}}(x, a, b) = \frac{c^3}{2\pi G} \frac{\sqrt{x-b}}{x^2 + a\sqrt{x-b}} \frac{\sqrt{\alpha_{\theta}}}{v_{\text{upp}}}, \quad (87)$$

where  $a = a_{3:2}^{\theta/r}(x, b)$  is given by the relation (77). Putting  $v_{\text{upp}} = v_{\theta}$ , we obtain the mass dependence of the spin assuming  $b = \text{const}$  (see Fig. 13). In a similar way, we obtain the relations  $M(x, a, b)$  for the relativistic precession model

$$M_{\text{RP}}(x, a, b) = \frac{c^3}{2\pi G} \frac{\sqrt{x-b}}{x^2 + a\sqrt{x-b}} \frac{1}{v_{\text{upp}}} \quad (88)$$

or Kato's warped disc trapped oscillation model

$$M_{\text{TO}}(x, a, b) = \frac{c^3}{2\pi G} \frac{\sqrt{x-b}}{x^2 + a\sqrt{x-b}} \frac{2 - \sqrt{\alpha_r}}{v_{\text{upp}}}, \quad (89)$$

putting  $v_{\text{upp}} \equiv v_K$  or  $v_{\text{upp}} \equiv 2v_K - v_r$ , respectively.

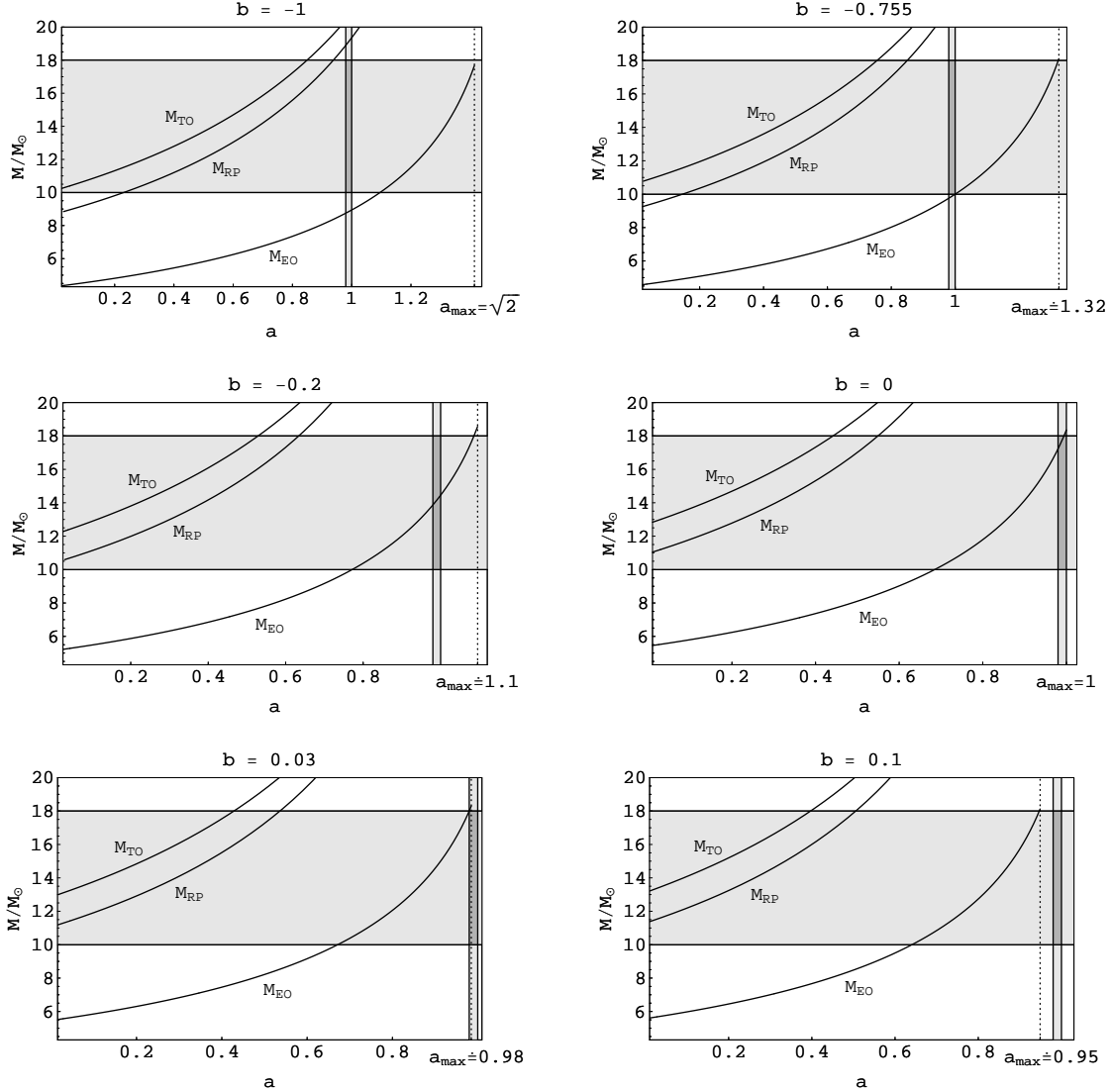


**Fig. 13** Possible combinations of mass and black hole spin predicted by the standard parametric epicyclic oscillations resonance model  $M_{EO}(a, b)$  with  $\nu_\theta : \nu_r = 3:2$ , the relativistic precession model  $M_{RP}(a, b)$  with  $\nu_K : (\nu_K - \nu_r) = 3:2$  and modified trapped oscillations model  $M_{TO}(a, b)$  with  $(2\nu_K - \nu_r) : 2(\nu_K - \nu_r) = 3:2$  for the high-frequency QPOs observed in the spectra of the microquasar GRS 1915+105. Shaded regions indicate the likely ranges for the mass (inferred from optical measurements of radial curves [52]) and the dimensionless spin (inferred from the X-ray spectral data fitting [51]) of GRS 1915+105.

Fig. 13 shows the predictions of the 3:2 parametric resonance model as well as the predictions of the relativistic precession and trapped oscillations models in the mass-spin plane. It demonstrates possible combinations of mass and black hole spin of GRS 1915+105 as they are predicted for various values of brany parameter  $b$ , considering the allowed range of the black hole mass.

It follows immediately from Fig. 13 that for all considered values of the brany parameter  $b$  the relativistic precession and the trapped oscillations models do not meet the observational data of GRS 1915+105 for the same spin as the parametric resonance model of epicyclic oscillations. Clearly, they can be applied for object with substantially lower spin.

According to the spectral analysis of the X-ray continuum by McClintock et al. [52], the compact primary of the binary X-ray source GRS 1915+105 is a rapidly-rotating Kerr black hole with a lower limit on its dimensionless spin of

$$a > 0.98. \quad (90)$$

We use this spin limit in Fig. 13.

Notice, however, that although the spectral fitting analysis has been done by McClintock et al. [52] very carefully, the spin estimate is valid only in the Kerr spacetime. We can suppose that for braneworld Kerr black hole with non-zero brany parameter  $b$ , the spin estimates may be shifted to higher (lower) values of  $a$  due to the influence of the brany tidal charge  $b < 0$  ( $b > 0$ ) on the optical phenomena near a rotating black hole [65, 64]. Therefore, using the optical phenomena modelling with brany parameter  $b$  included, we could expect stronger limits on allowed values of  $b$ .

## 7 Strong resonant phenomena – “magic” spin

Generally, the resonances could be excited at different radii of the accretion disc under different internal conditions; such a situation is discussed in detail by Stuchlík et al. [71]. However, we have shown [72] that for special resonant values of dimensionless black hole spin  $a$  strong resonant phenomena could occur when different resonances can be excited at the same radius, as cooperative phenomena between the resonances may work in such situations.

There exists a possibility of direct resonances of oscillations with all of the three orbital frequencies, characterized by a triple frequency ratio set

$$\nu_K : \nu_\theta : \nu_r = s : t : u \quad (91)$$

with  $s > t > u$  being small integers. The frequency set ratio (91) can be realized only for special resonant values of the black hole spin  $a$ . The black hole mass is then related to the magnitude of the frequencies.

Assuming two resonances  $\nu_K : \nu_\theta = s : t$  and  $\nu_K : \nu_r = s : u$  occurring at the same  $x$ , we arrive to the conditions

$$\alpha_\theta(a, b, x) = \left(\frac{t}{s}\right)^2, \quad (92)$$

$$\alpha_r(a, b, x) = \left(\frac{u}{s}\right)^2 \quad (93)$$

that have to be solved simultaneously for  $x$ ,  $a$  and  $b$ . The solution is given by the condition

$$a^\theta(x, b, t/s) = a^r(x, b, u/s), \quad (94)$$

where

$$a^\theta(x, b, t/s) = \frac{\sqrt{x-b}}{3x-2b} \left\{ 2x-b \pm \sqrt{b^2 - 2bx \left[ 2+x \left( \frac{t}{s} \right)^2 - 1 \right] + x^2 \left[ 4+3x \left( \frac{t}{s} \right)^2 - 1 \right]} \right\}, \quad (95)$$

$$a^r(x, b, u/s) = \frac{1}{3x-4b} \left\{ 4(x-b)^{3/2} \pm x \sqrt{b \left[ 3-4b \left( \frac{u}{s} \right)^2 \right] + x \left[ 7b \left( \frac{u}{s} \right)^2 - 2(2b+1) \right] - 3x^2 \left[ \left( \frac{u}{s} \right)^2 - 1 \right]} \right\}. \quad (96)$$

For Kerr spacetime with  $b = 0$  the explicit solution determining the relevant radius for any triple frequency set ratio  $s : t : u$  takes the form [72]

$$x(s, t, u) = \frac{6s^2}{6s^2 \pm 2\sqrt{2}\sqrt{(t-u)(t+u)(3s^2 - t^2 - 2u^2)} - (t^2 + 5u^2)}. \quad (97)$$

Clearly, the condition  $t^2 + 2u^2 \leq 3s^2$  is always satisfied. The corresponding special resonant black hole spin  $a$  is then determined, e.g., by Eq. (95) giving  $a^\theta(x(s, t, u), t/s)$ . Of course, we consider only the black hole cases when  $a \leq a_{\max}$ . This condition puts a restriction on allowed values of  $s, t, u$ . The function  $x(s, t, u)$  for  $b = 0$  is illustrated in Fig. 14 and the resonant points are given for  $5 \geq s > t > u$ . For  $b \neq 0$  the solutions are determined numerically and the results are given in Table 1 and Figs 15–17.

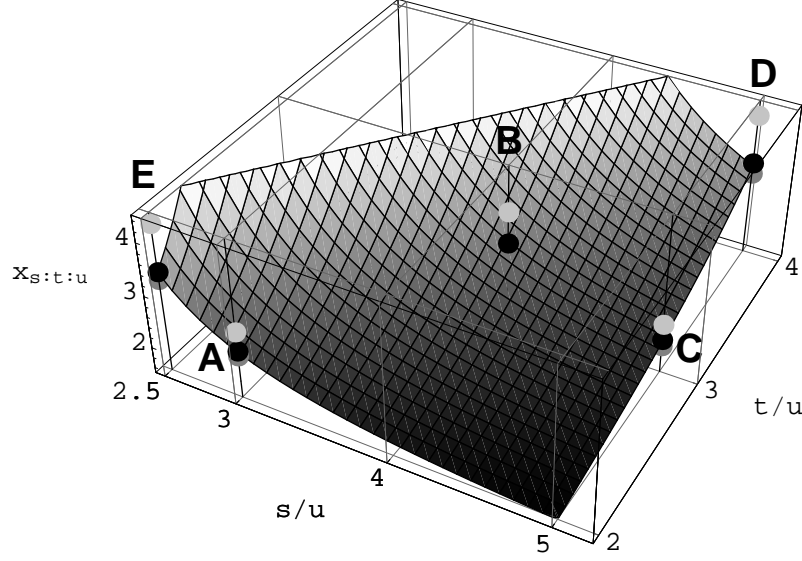


**Fig. 14** The function  $x(s/u, t/u)$  determining the triple frequency ratio set  $\nu_K : \nu_\theta : \nu_r = s : t : u$  at the same radius in Kerr black hole spacetime ( $b = 0$ ). The black points represent the ratios:  $s : t : u = 3 : 2 : 1$  (A),  $4 : 3 : 1$  (B),  $5 : 3 : 1$  (C),  $5 : 4 : 1$  (D),  $5 : 4 : 2$  (E) for  $b = 0$ , shaded points for  $b = 0.2$  and light shaded points for  $b = -2$ .

A detailed discussion of the black holes admitting strong resonant phenomena is for small integer ( $s \leq 5$ ) given in [72]. Of special interest seems to be the case of the “magic” spin, when the Keplerian and epicyclic frequencies are in the ratio  $\nu_K : \nu_\theta : \nu_r = 3 : 2 : 1$  at the shared resonance radius  $x_{3:2:1}$ . In fact, this case involves rather extended structure of resonances with  $\nu_K : \nu_r = 3 : 1$ ,  $\nu_K : \nu_\theta = 3 : 2$ ,  $\nu_\theta : \nu_r = 2 : 1$ . Notice that in this case also the simple combinational frequencies could be in this small integer ratio as

$$\frac{\nu_K}{\nu_\theta - \nu_r} = \frac{3}{1}, \quad \frac{\nu_K}{\nu_K - \nu_r} = \frac{3}{2}, \quad \frac{\nu_\theta}{\nu_\theta - \nu_r} = \frac{2}{1}. \quad (98)$$

Of course we obtain the strongest possible resonances when the beat frequencies enter the resonance satisfying the conditions

$$\frac{\nu_\theta + \nu_r}{\nu_K} = \frac{3}{3} = 1, \quad \frac{\nu_\theta}{\nu_K - \nu_r} = \frac{2}{2} = 1, \quad \frac{\nu_r}{\nu_K - \nu_\theta} = 1, \quad \frac{\nu_\theta - \nu_r}{\nu_r} = 1. \quad (99)$$

**Table 1** The intervals of the allowed values of the brany parameter  $b$  and the black hole spin  $a$  that imply the frequency ratio set  $\nu_K : \nu_\theta : \nu_r = s : t : u$  with  $5 \geq s > t > u$  at the shared radius. For some ratios such situation is possible only for naked singularity spacetimes (NaS).

$s : t : u$	$b_{s:t:u}$	$a_{s:t:u}$
3 : 2 : 1	-3.258 - +0.287	+0.844 - +2.063
4 : 2 : 1	only NaS	
4 : 3 : 1	-21.575 - +0.721	+0.528 - +4.751
4 : 3 : 2	only NaS	
5 : 2 : 1	only NaS	
5 : 3 : 1	-9.721 - +0.555	+0.667 - +3.274
5 : 3 : 2	only NaS	
5 : 4 : 1	$\leq 0.813$	$\geq 0.432$
5 : 4 : 2	-9.182 - +0.626	+0.612 - +3.191
5 : 4 : 3	only NaS	



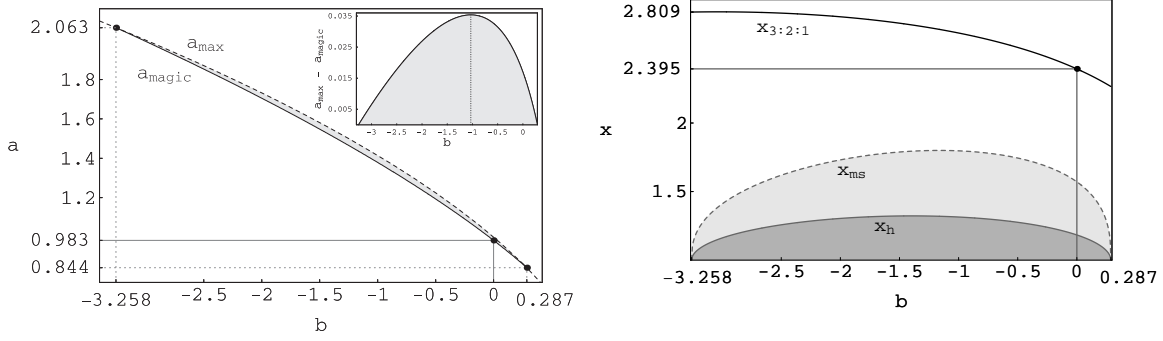


**Fig. 15** The “magic” black hole spin  $a$  (left panel) and the shared resonance radius  $x_{3:2:1}$  (right panel) as the function of the “magic” brany parameter  $b$  that imply the frequency ratio set  $\nu_K : \nu_\theta : \nu_r = 3 : 2 : 1$  arising at the shared radius  $x_{3:2:1}$ . Dashed line in the left panel represents  $a_{\max}$ , corresponding to the extreme black holes. We can see that for all possible values of the “magic” brany parameter  $a_{\text{magic}} \rightarrow a_{\max}$ . In the right panel, there is also shown the radius of the outer event black hole horizon  $x_h$  (gray solid line) and the marginally stable circular orbit  $x_{\text{ms}}$  (dashed line) of a rotating black hole carrying a given value of the “magic” brany parameter  $b$  and “magic” black hole spin  $a$ .

In the Kerr spacetimes, where  $b = 0$ , we obtain the “magic” spin  $a_{\text{magic}} = 0.983$  and the shared resonance radius  $x_{3:2:1} = 2.395$  (see Fig. 18). Assuming all possible values of brany parameter  $b$  we can conclude that this special case of the “magic” spin could occur only for brany parameter from the interval

$$b_{\text{magic}} \in \langle -3.258; 0.287 \rangle, \quad (100)$$

that implies the “magic” spin from the interval

$$a_{\text{magic}} \in \langle 0.844; 2.063 \rangle. \quad (101)$$

Only for these values of  $a$  and  $b$  we have  $a \leq a_{\max}$ , where  $a_{\max}$  corresponds to the extreme black hole (see Fig. 15).

### 7.1 Sgr A\* black hole parameters

The Galaxy center source Sgr A\* can serve as a proper candidate system, since three QPOs were reported (but not fully accepted by the astrophysical community) for the system [11, 76] with frequency ratio corresponding to the “magic” spin

$$(1/692) : (1/1130) : (1/2178) \approx 3 : 2 : 1 \quad (102)$$

and with the upper frequency being observed with a rather high error

$$\nu_{\text{upp}} = (1.445 \pm 0.16) \text{ mHz}. \quad (103)$$

Considering a black hole with the spin comparable to the “magic” value  $a \sim a_{\text{magic}}$ , with the frequency ratio  $\nu_K : \nu_\theta : \nu_r = 3 : 2 : 1$  at the shared resonance radius  $x_{3:2:1}$ , and identifying  $\nu_{\text{upp}} = \nu_K$ , we obtain for all possible values of “magic” brany parameter  $b_{\text{magic}} \in \langle -3.258; 0.287 \rangle$  the black hole mass of Sgr A\* in the interval

$$3.82 \times 10^6 M_\odot < M < 5.59 \times 10^6 M_\odot, \quad (104)$$

which meets the allowed range of the Sgr A\* mass coming from the analysis of the orbits of stars moving within 1000 light hours of Sgr A\* [30]

$$2.8 \times 10^6 M_\odot < M < 4.6 \times 10^6 M_\odot \quad (105)$$

at its higher mass end. In all these cases, the black hole spin  $a \rightarrow a_{\max}$ , in agreement with the assumption that Galactic center black hole should be fast rotating. The results are summarized in Table 2.

From Fig. 19 we can see that the best fit is obtained for the brany parameter  $b \sim -2.97$  that implies “magic” spin  $a_{\text{magic}} \sim 1.99$  and the radius  $x_{3:2:1} = 2.81$ .

The model should be further tested and more precise frequency measurements are very important for better fits of the models and observational data.

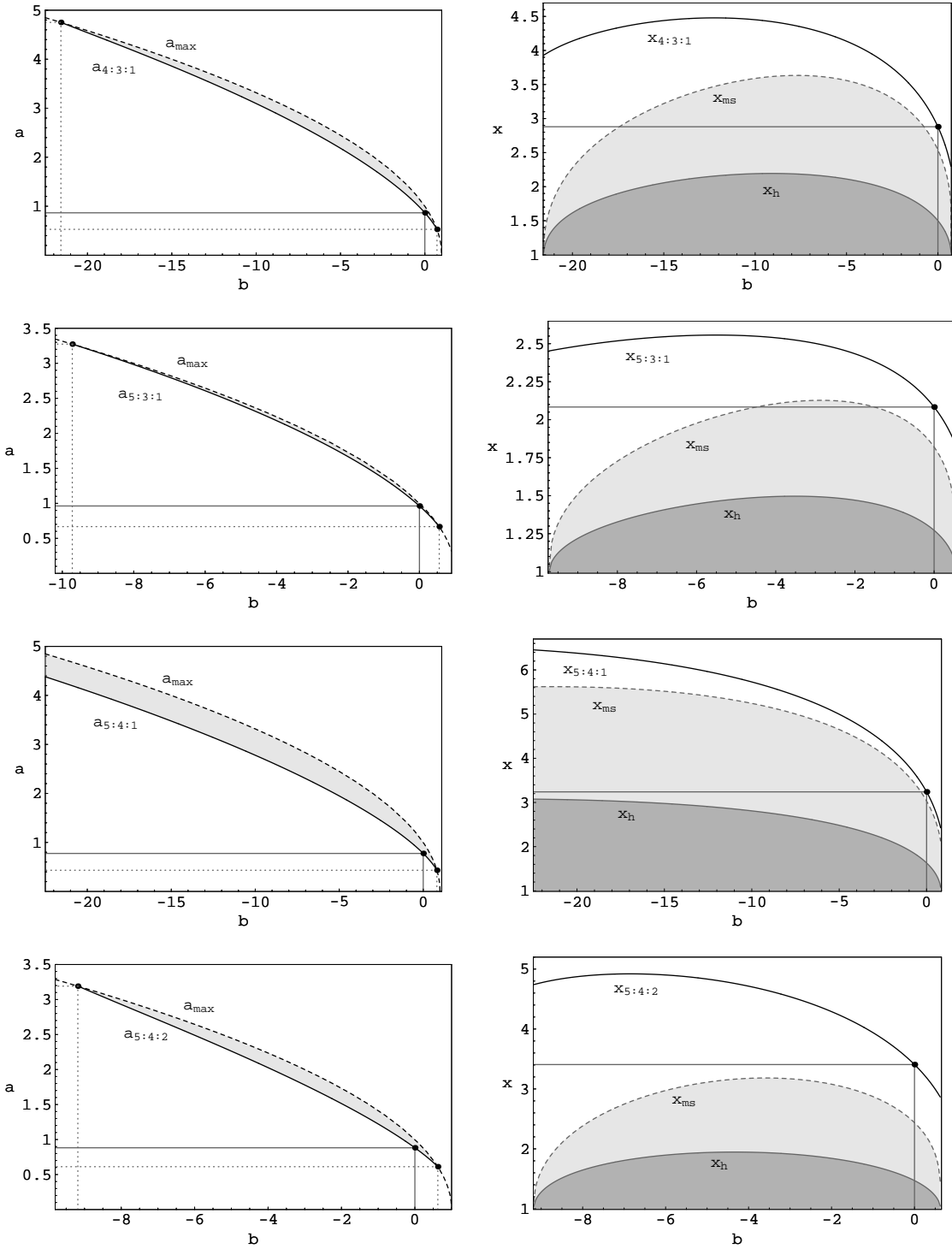


**Fig. 16** The black hole spin  $a$  (left panel) and the shared resonance radius  $x_{s:t:u}$  (right panel) as the function of the brany parameter  $b$  that imply the frequency ratio set  $\nu_K : \nu_\theta : \nu_r = s:t:u$  arising at the same radius  $x_{s:t:u}$  for  $s:t:u = 4:3:1, 5:3:1, 5:4:1$  and  $5:4:2$ .

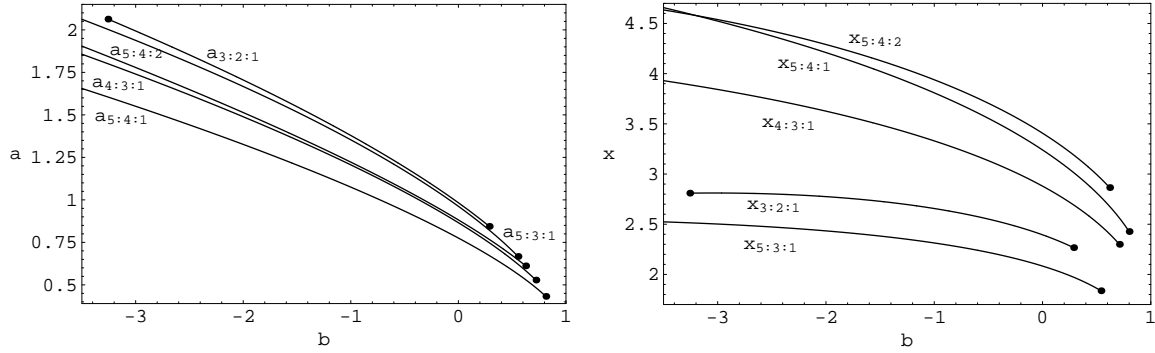


**Fig. 17** The black hole spin (*left panel*) and the shared resonance radius (*right panel*) for the ratios  $\nu_K : \nu_\theta : \nu_r = s : t : u$  with integers  $\leq 5$  allowed in the field of brany Kerr black holes.

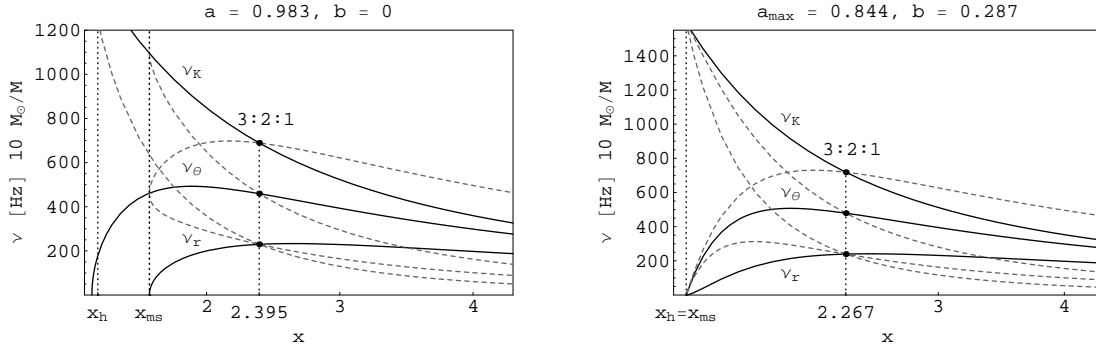


**Fig. 18** The special cases of the “magic” black hole spin  $a$  enabling presence of strong resonant phenomena at the radius where  $\nu_K : \nu_\theta : \nu_r = 3 : 2 : 1$  for Kerr spacetime (*left panel*) and for braneworld black hole with the extreme  $b = 0.287$  (*right panel*). For completeness we present the relevant simple combinational frequencies  $\nu_\theta - \nu_r$ ,  $\nu_\theta + \nu_r$ ,  $\nu_K - \nu_\theta$ ,  $\nu_K - \nu_r$  (grey dashed lines). Notice that the “magic” spin represents the only case when the combinational and direct orbital frequencies coincide at the shared resonance radius.

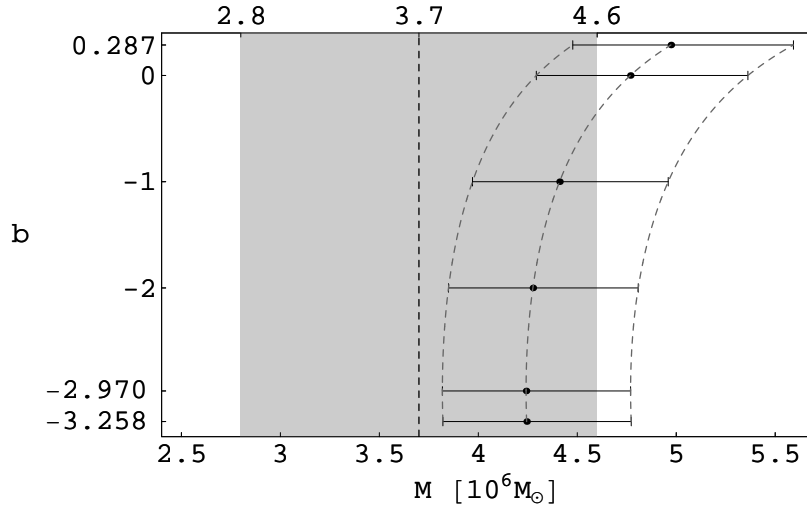


**Fig. 19** Mass of Sgr A\*: strong resonant model with the frequency ratio  $\nu_K : \nu_\theta : \nu_r = 3 : 2 : 1$  for various values of brany parameter  $b$ . The observational restrictions from the orbital motion of stars in vicinity of Sgr A\* [30] are illustrated here by the gray rectangle.

**Table 2** Determining of the black hole spin and mass in Sgr A\* with assumed observed characteristic frequency ratio set  $\nu_K : \nu_\theta : \nu_r = 3:2:1$  at the shared resonance radius  $x_{3:2:1}$  for various values of brany parameter  $b$ ;  $\nu_{\text{upp}} = (1.445 \pm 0.16)$  mHz is used to determine the black hole mass.

$b_{\text{magic}}$	$a_{\text{magic}}$	$x_{\text{ms}}$	$x_{3:2:1}$	$M [10^6 M_\odot]$
0.287150	0.844304	1	2.26663	4.477 – 5.592
0	0.983043	1.57081	2.39467	4.293 – 5.362
-1	1.378867	1.79706	2.65656	3.971 – 4.959
-2	1.705166	1.73104	2.77498	3.849 – 4.808
-2.969659	1.985138	1.42803	2.81093	3.819 – 4.769
-3.257659	2.063410	1	2.80953	3.821 – 4.773

## 8 Conclusions

The orbital resonance model and its simple generalization to multiresonance model with strong resonances is formulated for the brany Kerr black holes, when the bulk-space influence is described by a single, brany tidal charge parameter.

In the limit of strong gravitational field, the brany parameter  $b$  can be, in principle, high in its magnitude, therefore, we put no restriction on the values of  $b$ . We describe the properties of the radial and vertical epicyclic frequencies related to the oscillatory motion in the equatorial plane of the Kerr spacetimes. While their behaviour is qualitatively similar for Kerr and brany Kerr black holes, there are strong differences in the case of naked singularities – in some range of their parameters, the vertical epicyclic frequency could be even lower than the radial one. Such a situation is impossible in standard Kerr spacetimes. Further, in the field of brany Kerr naked singularities, the structure of the radial profiles is much richer than in the standard case, namely the number of local extrema could be higher in comparison with the standard Kerr naked singularities. In a special family of the brany naked singularity spacetimes, the radial epicyclic frequency has no zero point since there is no marginally stable circular geodesic in these spacetimes.

Assuming the parametric resonance acting directly between the oscillations with radial and vertical epicyclic frequency [80], we give the rule for the resonant radius with a given frequency ratio. The rule is tested for the uppermost twin frequencies observed in the GRS 1915+105 microquasar; and limits on the spin and brany parameters are obtained and compared with the estimates for  $b = 0$ , given in [80].<sup>7</sup> Further, it is shown that the relativistic precession model [69] and the trapped oscillations of warped disc model [38,37] are not able to fit the observational data of GRS 1915+105, with high spin limits, as these two models work well for small or mediate black hole spin.

In the Galaxy center source Sgr A\*, three frequencies were reported [11,12,76,77] that could be treated in the scope of the strong resonance model. The model predicts an exact value of the black hole spin and puts limits on its mass. It is shown that the black hole mass estimate given by the strong resonance model is in the best agreement with the value of  $M \sim 3.7 \times 10^6 M_\odot$  [30] for negative brany parameter  $b \sim -2.97$ , with the “magic” spin  $a \approx 1.99$ . Generally, for negative values of  $b$  the fit of the model with observational data is better than for  $b = 0$ , while for positive values of  $b$  the inverse holds.

Our resonance models could be to some extent applied to slowly rotating neutron stars, when the Kerr metric could be relevant, and there are some indications that orbital resonance models could be relevant to explain also the data from binary neutron star systems [78,85,82,79].

We can conclude that the orbital resonance model and its generalization to the multiresonant model is able to put some astrophysically interesting limits on the values of the brany parameter and could be useful in estimating influence of hypothetical external dimension to the properties of the brany universe.

**Acknowledgements** This work was supported by the Czech grant MSM 4781305903. One of the authors (Zdeněk Stuchlík) would like to express his gratitude to the Czech Committee for Collaboration with CERN for support and Theory Division CERN for perfect hospitality.

<sup>7</sup> However, it should be noted that whole the five frequency pattern can be explained in the framework of the extended resonance model assuming near-extreme Kerr black holes [16,68,75,74,73].

---

**References**

1. Abramowicz, M.A., Barret, D., Bursa, M., Horák, J., Kluźniak, W., Rebusco, P., Török, G.: A note on the slope-shift anticorrelation in the neutron star kHz QPOs data. In: Hledík and Stuchlík [33], pp. 1–9
2. Abramowicz, M.A., Barret, D., Bursa, M., Horák, J., Kluźniak, W., Rebusco, P., Török, G.: The correlations and anticorrelations in QPO data. *Astronom. Nachr.* **326**(9), 864–866 (2005), arXiv:astro-ph/0510462v1
3. Abramowicz, M.A., Chen, X., Kato, S., Lasota, J.P., Regev, O.: Thermal equilibria of accretion disks. *Astrophys. J.* **438**, L37–L39 (1995), arXiv:astro-ph/9409018v1
4. Abramowicz, M.A., Kluźniak, W.: A precise determination of black hole spin in GRO J1655–40. *Astronomy and Astrophysics* **374**, L19 (2001), arXiv:astro-ph/0105077v1
5. Abramowicz, M.A., Kluźniak, W., Stuchlík, Z., Török, G.: Twin peak QPOs frequencies in microquasars and Sgr A\*. The resonance and other orbital models. In: Hledík and Stuchlík [32], pp. 1–23
6. Aliev, A.N., Galtsov, D.V.: Radiation from relativistic particles in nongeodesic motion in a strong gravitational field. *General Relativity and Gravitation* **13**, 899–912 (1981)
7. Aliev, A.N., Gümrukçüoğlu, A.E.: Gravitational Field Equations on and off a 3-Brane World. *Classical Quantum Gravity* **21**, 5081 (2004), arXiv:hep-th/0407095v1
8. Aliev, A.N., Gümrukçüoğlu, A.E.: Charged rotating black holes on a 3-brane. *Phys. Rev. D* **71**(10), 104,027 (2005), arXiv:hep-th/0502223v2
9. Arkani-Hamed, N., Dimopoulos, S., Dvali, G.: The Hierarchy Problem and New Dimensions at a Millimeter. *Phys. Lett. B* **429**, 263–272 (1998), arXiv:hep-ph/9803315v1
10. Arnowitt, R., Deser, S., Misner, C.W.: The Dynamics of General Relativity. L. Witten ed. (Wiley 1962) **7**, 227–265 (1962), arXiv:gr-qc/0405109v1
11. Aschenbach, B.: Measuring mass and angular momentum of black holes with high-frequency quasi-periodic oscillations. *Astronomy and Astrophysics* **425**, 1075–1082 (2004), arXiv:astro-ph/0406545v1
12. Aschenbach, B.: Measurement of Mass and Spin of Black Holes with QPOs. *Chin. J. Astron. Astrophys.* (2007), accepted, arXiv:0710.3454v1 [astro-ph]
13. Aschenbach, B., Grosso, N., Porquet, D., Predehl, P.: X-ray flares reveal mass and angular momentum of the Galactic Center black hole. *Astronomy and Astrophysics* **417**, 71–78 (2004), arXiv:astro-ph/0401589v2
14. Bakala, P., Šrámková, E., Stuchlík, Z., Török, G.: On magnetic-field induced non-geodesic corrections to the relativistic precession QPO model. *Astrophys. J.* (2008), submitted
15. Bardeen, J.M.: Timelike and null geodesics in the Kerr metric. In: C.D. Witt, B.S.D. Witt (eds.) *Black Holes*, p. 215. Gordon and Breach, New York–London–Paris (1973)
16. Blaes, O.M., Šrámková, E., Abramowicz, M.A., Kluźniak, W., Torkelsson, U.: Epicyclic Oscillations of Fluid Bodies: Newtonian Nonslender Torus. *Astrophys. J.* **665**, 642–653 (2007), arXiv:0706.4483v1 [astro-ph]
17. Böhmer, C.G., Harko, T., Lobo, F.S.N.: Solar system tests of brane world models. *Classical Quantum Gravity* **25**(4), 5015 (2008), arXiv:0801.1375v2 [gr-qc]
18. Carter, B.: Global Structure of the Kerr Family of Gravitational Fields. *Phys. Rev.* **174**(5), 1559–1571 (1968)
19. Carter, B.: Black hole equilibrium states. In: C.D. Witt, B.S.D. Witt (eds.) *Black Holes*, pp. 57–214. Gordon and Breach, New York–London–Paris (1973)
20. Chamblin, A., Hawking, S.W., Reall, H.S.: Brane-World Black Holes. *Phys. Rev. D* **61**(6), 065,007 (2000), arXiv:hep-th/9909205v2
21. Chamblin, A., Reall, H.S., Shinkai, H.A., Shiromizu, T.: Charged Brane-World Black Holes. *Phys. Rev. D* **63**(6), 064,015 (2001), arXiv:hep-th/0008177v2
22. Dadhich, N., Kale, P.P.: Equatorial circular geodesics in the Kerr–Newman geometry. *J. Math. Phys.* **18**, 1727–1728 (1977)
23. Dadhich, N., Maartens, R., Papadopoulos, P., Rezanian, V.: Black holes on the brane. *Phys. Lett. B* **487**, 1 (2000), arXiv:hep-th/0003061v3
24. Damour, T., Hanni, R.S., Ruffini, R., Wilson, J.R.: Regions of magnetic support of a plasma around a black hole. *Phys. Rev. D* **17**(6), 1518–1523 (1978)
25. Dimopoulos, S., Landsberg, G.: Black Holes at the Large Hadron Collider. *Phys. Rev. Lett.* **87**(16), 161,602 (2001), arXiv:hep-ph/0106295v1
26. Dovčiak, M., Karas, V., Martocchia, A., Matt, G., Yaqoob, T.: An XSPEC model to explore spectral features from black-hole sources. In: Hledík and Stuchlík [32], pp. 33–73, arXiv:astro-ph/0407330v1
27. Emparan, R., Masip, M., Rattazzi, R.: Cosmic Rays as Probes of Large Extra Dimensions and TeV Gravity. *Phys. Rev. D* **65**, 064,023 (2002), arXiv:hep-ph/0109287v2
28. Fabian, A.C., Miniutti, G.: *Kerr Spacetime: Rotating Black Holes in General Relativity*. Cambridge University Press, Cambridge (2005). Eprint arXiv:astro-ph/0507409v1 is a part of this book
29. Germani, C., Maartens, R.: Stars in the braneworld. *Phys. Rev. D* **64**, 124,010 (2001), arXiv:hep-th/0107011v3
30. Ghez, A.M., Salim, S., Hornstein, S.D., Tanner, A., Lu, J.R., Morris, M., Becklin, E.E., Duchêne, G.: Stellar Orbits around the Galactic Center Black Hole. *Astrophys. J.* **620**, 744–757 (2005), arXiv:astro-ph/0306130v2
31. Gregory, R., Laflamme, R.: Black Strings and p-Branes are Unstable. *Phys. Rev. Lett.* **70**(19), 2837–2840 (1993), arXiv:hep-th/9301052v2
32. Hledík, S., Stuchlík, Z. (eds.): Proceedings of RAGtime 4/5: Workshops on black holes and neutron stars, Opava, 14–16/13–15 October 2002/2003. Silesian University in Opava, Opava (2004)
33. Hledík, S., Stuchlík, Z. (eds.): Proceedings of RAGtime 6/7: Workshops on black holes and neutron stars, Opava, 16–18/18–20 September 2004/2005. Silesian University in Opava, Opava (2005)
34. Hledík, S., Stuchlík, Z. (eds.): Proceedings of RAGtime 8/9: Workshops on black holes and neutron stars, Opava, Hradec nad Moravicí, 15–19/19–21 September 2006/2007. Silesian University in Opava, Opava (2007)
35. Horowitz, G.T., Maeda, K.: Fate of the Black String Instability. *Phys. Rev. Lett.* **87**(13), 131,301 (2001), arXiv:hep-th/0105111v2

36. Karas, V., Vokrouhlický, D., Polnarev, A.G.: In the vicinity of a rotating black hole – A fast numerical code for computing observational effects. *Monthly Notices Roy. Astronom. Soc.* **259**, 569–575 (1992)
37. Kato, S.: Resonant Excitation of Disk Oscillations by Warps: A Model of kHz QPOs. *Publ. Astronom. Soc. Japan* **56**(5), 905–922 (2004), arXiv:astro-ph/0409051v2
38. Kato, S.: Frequency Correlations of QPOs Based on a Disk Oscillation Model in Warped Disks. *Publ. Astronom. Soc. Japan* **59**, 451–455 (2007), arXiv:astro-ph/0701085v1
39. Kato, S., Fukue, J., Mineshige, S.: Black-hole accretion disks. In: S. Kato, J. Fukue, S. Mineshige (eds.) *Black-hole accretion disks*. Kyoto University Press, Kyoto, Japan (1998)
40. Keeton, C.R., Petters, A.O.: Formalism for testing theories of gravity using lensing by compact objects. III. Braneworld gravity. *Phys. Rev. D* **73**(10), 104,032 (2006), arXiv:gr-qc/0603061v3
41. van der Klis, M.: Millisecond Oscillations in X-ray Binaries. *Annual Review of Astronomy and Astrophysics* **38**, 717–760 (2000), arXiv:astro-ph/0001167v1
42. van der Klis, M.: Rapid X-ray Variability. In: W.H.G. Lewin, M. van der Klis (eds.) *Compact Stellar X-Ray Sources*, pp. 39–112. Cambridge University Press, Cambridge (2006)
43. Kluźniak, W., Abramowicz, M.A., Bursa, M., Török, G.: QPOs and Resonance in Accretion Disks. In: W.H. Lee, E. Ramírez-Ruiz (eds.) *Revista Mexicana de Astronomía y Astrofísica (Serie de Conferencias)*, vol. 27, pp. 18–25 (2007)
44. Kozłowski, M., Jaroszyński, M., Abramowicz, M.A.: The analytic theory of fluid disks orbiting the Kerr black hole. *Astronomy and Astrophysics* **63**(1–2), 209–220 (1978)
45. Krolik, J.H., Hawley, J.F.: Where Is the Inner Edge of an Accretion Disk around a Black Hole? *Astrophys. J.* **573**(2), 754–763 (2002), arXiv:astro-ph/0203289v1
46. Lachowicz, P., Czerny, B., Abramowicz, M.A.: Wavelet analysis of MCG-6-30-15 and NGC 4051: a possible discovery of QPOs in 2:1 and 3:2 resonance. *Monthly Notices Roy. Astronom. Soc.* (2006), submitted, arXiv:astro-ph/0607594v1
47. Landau, L.D., Lifshitz, E.M.: *Mechanics, Course of Theoretical Physics*, vol. I, 3rd edn. Elsevier Butterworth-Heinemann, Oxford (1976)
48. Laor, A.: Line profiles from a disk around a rotating black hole. *Astrophys. J.* **376**, 90–94 (1991)
49. Maartens, R.: Brane-world gravity. *Living Rev. Rel.* **7**, 7 (2004), arXiv:gr-qc/0312059v2
50. McClintock, J.E., Narayan, R., Shafee, R.: Estimating the Spins of Stellar-Mass Black Holes. In: M. Livio, A. Koekemoer (eds.) *Black Holes*. Cambridge University Press, Cambridge (2007), in press, arXiv:0707.4492v1 [astro-ph]
51. McClintock, J.E., Remillard, R.A.: Black Hole Binaries. In: W.H.G. Lewin, M. van der Klis (eds.) *Compact Stellar X-Ray Sources*. Cambridge University Press, Cambridge (2004), arXiv:astro-ph/0306213v4
52. McClintock, J.E., Shafee, R., Narayan, R., Remillard, R.A., Davis, S.W., Li, L.X.: The Spin of the Near-Extreme Kerr Black Hole GRS 1915+105. *Astrophys. J.* **652**, 518–539 (2006), arXiv:astro-ph/0606076v2
53. Middleton, M., Done, C., Gierliński, M., Davis, S.W.: Black hole spin in GRS 1915+105. *Monthly Notices Roy. Astronom. Soc.* **373**, 1004–1012 (2006), arXiv:astro-ph/0601540v2
54. Misner, C.W., Thorne, K.S., Wheeler, J.A.: *Gravitation*. W. H. Freeman and Co, New York, San Francisco (1973)
55. Modgil, M.S., Panda, S., Sengupta, G.: Rotating Brane World Black Holes. *Modern Phys. Lett. A* **17**, 1479–1487 (2002), arXiv:hep-th/0104122v2
56. Narayan, R., Yi, I.: Advection-dominated accretion: A self-similar solution. *Astrophys. J.* **428**, L13–L16 (1994), arXiv:astro-ph/9403052v1
57. Nojiri, S., Obregon, O., Odintsov, S.D., Ogushi, S.: Dilatonic Brane-World Black Holes, Gravity Localization and Newton’s Constant. *Phys. Rev. D* **62**(6), 064,017 (2000), arXiv:hep-th/0003148v1
58. Novikov, I.D., Thorne, K.S.: Black hole astrophysics. In: C.D. Witt, B.S.D. Witt (eds.) *Black Holes*, p. 343. Gordon and Breach, New York–London–Paris (1973)
59. Randall, L., Sundrum, R.: An Alternative to Compactification. *Phys. Rev. Lett.* **83**(23), 4690–4693 (1999), arXiv:hep-th/9906064v1
60. Remillard, R.A.: X-ray spectral states and high-frequency QPOs in black hole binaries. *Astronom. Nachr.* **326**(9), 804–807 (2005), arXiv:astro-ph/0510699v1
61. Remillard, R.A., McClintock, J.E.: X-Ray Properties of Black-Hole Binaries. *Annual Review of Astronomy and Astrophysics* **44**(1), 49–92 (2006), arXiv:astro-ph/0606352v1
62. Rezzolla, L., Yoshida, S., Maccarone, T.J., Zanutti, O.: A new simple model for high-frequency quasi-periodic oscillations in black hole candidates. *Monthly Notices Roy. Astronom. Soc.* **344**(3), L37–L41 (2003), arXiv:astro-ph/0307487v1
63. Sasaki, M., Shiromizu, T., Maeda, K.-i.: Gravity, stability, and energy conservation on the Randall–Sundrum brane world. *Phys. Rev. D* **62**, 024,008 (2000), arXiv:hep-th/9912233v3
64. Schee, J., Stuchlík, Z.: Optical effects in brany Kerr spacetimes. In: Hledík and Stuchlík [34], pp. 221–256
65. Schee, J., Stuchlík, Z.: Spectral line profile of radiating ring orbiting a brany Kerr black hole. In: Hledík and Stuchlík [34], pp. 209–220
66. Shafee, R., McClintock, J.E., Narayan, R., Davis, S.W., Li, L.X., Remillard, R.A.: Estimating the Spin of Stellar-Mass Black Holes by Spectral Fitting of the X-Ray Continuum. *Astrophys. J.* **636**, L113–L116 (2006), arXiv:astro-ph/0508302v2
67. Shiromizu, T., Maeda, K.-i., Sasaki, M.: The Einstein Equations on the 3-Brane World. *Phys. Rev. D* **62**, 024,012 (2000), arXiv:gr-qc/9910076v3
68. Šrámková, E.: Epicyclic oscillation modes of a Newtonian, non-slender torus. *Astronom. Nachr.* **326**(9), 835–837 (2005)
69. Stella, L., Vietri, M.: Lense–Thirring Precession and Quasi-periodic Oscillations in Low-Mass X-Ray Binaries. *Astrophys. J. Lett.* **492**, L59–L62 (1998), arXiv:astro-ph/9709085v1
70. Strohmayer, T.E., Mushotzky, R., Winter, L., Soria, R., Uttley, P., Cropper, M.: Quasi-periodic Variability in NGC 5408 X-1. *Astrophys. J.* **660**, 580–586 (2007), arXiv:astro-ph/0701390v1
71. Stuchlík, Z., Kotrlová, A., Török, G.: Multi-resonance models of QPOs. In: Hledík and Stuchlík [34], pp. 363–416
72. Stuchlík, Z., Kotrlová, A., Török, G.: Black holes admitting strong resonant phenomena. *Acta Astronom.* (2008), accepted, arXiv:0812.4418v1 [astro-ph]
73. Stuchlík, Z., Slaný, P., Török, G.: Extended orbital resonance model with hump-induced oscillations. In: Hledík and Stuchlík [34], pp. 449–467

- 
74. Stuchlík, Z., Slaný, P., Török, G.: Humpy LNRF-velocity profiles in accretion discs orbiting almost extreme Kerr black holes – A possible relation to quasi-periodic oscillations. *Astronomy and Astrophysics* **463**(3), 807–816 (2007), arXiv:astro-ph/0612439v1
  75. Stuchlík, Z., Slaný, P., Török, G.: LNRF-velocity hump-induced oscillations of a Keplerian disc orbiting near-extreme Kerr black hole: a possible explanation of high-frequency QPOs in GRS 1915+105. *Astronomy and Astrophysics* **470**, 401–404 (2007), arXiv:0704.1252v2 [astro-ph]
  76. Török, G.: A possible 3:2 orbital epicyclic resonance in QPOs frequencies of Sgr A\*. *Astronomy and Astrophysics* **440**(1), 1–4 (2005), arXiv:astro-ph/0412500v1
  77. Török, G.: QPOs in microquasars and Sgr A\*: measuring the black hole spin. *Astronom. Nachr.* **326**(9), 856–860 (2005), arXiv:astro-ph/0510669v1
  78. Török, G.: Reverse of twin peak QPO amplitude relationship in six atoll sources. *Astronomy and Astrophysics* (2008), submitted
  79. Török, G., Abramowicz, M.A., Bakala, P., Bursa, M., Horák, J., Rebusco, P., Stuchlík, Z.: On the origin of clustering of frequency ratios in the atoll source 4U 1636–53. *Acta Astronom.* **58**, 113–119 (2008), arXiv:0802.4026v2 [astro-ph]
  80. Török, G., Abramowicz, M.A., Kluźniak, W., Stuchlík, Z.: The orbital resonance model for twin peak kHz quasi periodic oscillations in microquasars. *Astronomy and Astrophysics* **436**(1), 1–8 (2005), arXiv:astro-ph/0401464v1
  81. Török, G., Abramowicz, M.A., Stuchlík, Z., Šrámková, E.: QPOs in microquasars: the spin problem. In: W.I. Hartkopf, E.F. Guinan, P. Harmanec (eds.) *IAU Symposium*, vol. 240, pp. 724–726 (2007), arXiv:astro-ph/0610497v1
  82. Török, G., Bakala, P., Stuchlík, Z., Čech, P.: Modelling the twin peak QPO distribution in the atoll source 4U 1636–53. *Acta Astronom.* **58**, 1–14 (2008)
  83. Török, G., Stuchlík, Z.: Epicyclic frequencies of Keplerian motion in Kerr spacetimes. In: Hledík and Stuchlík [33], pp. 315–338
  84. Török, G., Stuchlík, Z.: Radial and vertical epicyclic frequencies of Keplerian motion in the field of Kerr naked singularities. Comparison with the black hole case and possible instability of naked singularity accretion discs. *Astronomy and Astrophysics* **437**(3), 775–788 (2005), arXiv:astro-ph/0502127v1
  85. Török, G., Stuchlík, Z., Bakala, P.: A remark about possible unity of the neutron star and black hole high frequency QPOs. *Central European J. Phys.* **5**(4), 457–462 (2007)
  86. Zakharov, A.F.: The iron  $K_{\alpha}$  line as a tool for analysis of black hole characteristics. *Publications of the Astronomical Observatory of Belgrade* **76**, 147–162 (2003), arXiv:astro-ph/0411611v1
  87. Zakharov, A.F., Repin, S.V.: Different types of Fe  $K_{\alpha}$  lines from radiating annuli near black holes. *New Astronomy* **11**, 405–410 (2006), arXiv:astro-ph/0510548v1
  88. Zel'dovich, Y.B., Novikov, I.D.: *Relativistic Astrophysics*, vol. 1. University of Chicago Press, Chicago (1971)